

The role of plasminogen LBS in binding to nicked  $\beta_2$ -GPI was evaluated by a competitive ELISA adding serial dilutions of EACA, a lysine analog, into the nicked  $\beta_2$ -GPI solution.

**Kinetic assay for molecular interaction between nicked  $\beta_2$ -GPI and plasminogen.** Real-time analysis for molecular interaction between nicked  $\beta_2$ -GPI and Glu-plasminogen was performed using an optical-biosensor, LAsys system (Affinity Sensors, Paramus, NJ). Biotinylated Glu-plasminogen was immobilized on the wall of a biotin cuvette (Affinity Sensors) via streptavidin (Sigma Chemical). After blocking with 0.01% BSA-PBS and washing with PBS, various concentrations (up to 4  $\mu$ M) of native or nicked  $\beta_2$ -GPI were placed in the cuvette and ligand bound to the plasminogen-coated surface was detected. Obtained data were fitted using linear regression to find the intercept and gradient. This analysis was used to determine the association rate constant ( $k_{on}$ ) and dissociation rate constant ( $k_{off}$ ), from the variation of the on-rate constant ( $k_{on}$ ) with ligand concentration. According to the equation:  $k_{on} = k_{diss} + k_{ass}[\text{ligand}]$ ,  $k_{on}$  and  $k_{off}$  are determined as follows:  $K_D = k_{diss}/k_{ass}$  and  $K_A = k_{ass}/k_{diss}$ .

**Inhibition ELISA.** To identify the nicked  $\beta_2$ -GPI-binding site on Glu-plasminogen, the inhibition of Glu-plasminogen binding by fragments of plasminogen was examined. Fifty microliters of nicked  $\beta_2$ -GPI (0.2  $\mu$ M) diluted in PBS was put into each well of a MaxiSorp microtiter plate (Nalge Nunc International, Roskilde, Denmark) and incubated overnight at 4°C. After washing twice with PBS and blocking with 2% gelatin-PBS for 1 hour at 37°C, serial dilutions of inhibitor (BSA, plasminogen kringle 1-3, plasminogen kringle 4, or mini-plasminogen) were added (50  $\mu$ L/well) followed by overnight incubation at 4°C. After washing with PBS-Tween, 10  $\mu$ g/mL Glu-plasminogen was then added (50  $\mu$ L/well) and incubated for 30 minutes at room temperature, and plates were washed 3 times with PBS-Tween. To compare the inhibitory effect between kringle 1 to 3 and mini-plasminogen, a monoclonal antikringle 4 antibody (American Diagnostica) was used to detect bound Glu-plasminogen, whereas a monoclonal antikringle 1 to 3 antibody (American Diagnostica) was used to compare the inhibition of mini-plasminogen with that of kringle 4. After incubation with these monoclonal antibodies, bound Glu-plasminogen on nicked  $\beta_2$ -GPI was evaluated by ALP-conjugated antimouse IgG, followed by substrate addition as described ("ELISA for binding of intact or nicked  $\beta_2$ -GPI to plasminogen").

**Inhibitory effect of nicked  $\beta_2$ -GPI on the binding of plasminogen to fibrin.** To investigate whether nicked  $\beta_2$ -GPI interferes with the binding of Glu-plasminogen to immobilized fibrin in a liquid phase or not, the following experiment was done. Each well of a Sumilon Type S microtiter plate (Sumitomo Bakelite) was coated with soluble fibrin monomer (5  $\mu$ g/mL) and incubated at 4°C overnight, followed by washing with PBS-Tween and blocking with 2% gelatin-PBS at 37°C. Biotinylated Glu-plasminogen (5  $\mu$ g/mL in 1% BSA-PBS) was preincubated with different concentrations of intact or nicked  $\beta_2$ -GPI for 1 hour at room temperature and added to the wells in triplicate. After incubation for 1 hour at room temperature, each well was washed with PBS-Tween. ALP-conjugated streptavidin was diluted to 3000 times in PBS and distributed to the wells. After 1 hour of incubation and washing, substrate was added and absorbance was measured as described.

**Effects of intact or nicked  $\beta_2$ -GPI on tPA activity: chromogenic assay.** In the presence of fibrin, tPA can effectively activate plasminogen to plasmin. Because we speculated that nicked  $\beta_2$ -GPI might interfere with this activation step by binding to plasminogen, chromogenic assay measuring plasmin generation was introduced in the presence of tPA. Glu-plasminogen, fibrin monomer, and  $\beta_2$ -GPI. The effect of intact/nicked  $\beta_2$ -GPI on the activity of plasmin generated was evaluated using a parabolic rate assay. The activity of tPA was measured in a chromogenic assay as described<sup>27</sup> with some modifications. A mixture of the same volume of 50 U/mL tPA in PBS and 1 M acetate buffer (pH 3.9) was incubated for 5 minutes at room temperature, then diluted 1:160 with assay buffer (50 mM Tris-HCl, pH 8.8, 100 mM NaCl, and 0.01% Triton X-100). Then 100  $\mu$ L of the diluted tPA solution was incubated in a Sumilon Type S microtiter plate with 100  $\mu$ L detection reagents consisting of Glu-plasminogen and plasmin-sensitive substrate (Glu-plasminogen [70  $\mu$ g/mL] and 0.6 mM chromogenic substrate S-2251 [Chromogenix, Möndal, Sweden] in assay buffer) with intact or nicked  $\beta_2$ -GPI and 2  $\mu$ L/well soluble fibrin monomer

(3.3 mg/mL, in 3.5 M urea). The final concentrations of intact/nicked  $\beta_2$ -GPI were 0, 0.25, and 0.5  $\mu$ M. Domain I to IV of  $\beta_2$ -GPI mutant or BSA served as the negative control. After incubation at 37°C for 12 hours, the activity of plasmin generated was determined by measuring absorbance at 405 nm using a microplate reader (model 3550; BioRad, Hercules, CA). A standard curve was generated using serial dilutions of tPA. The plasmin generation in this system was expressed as corresponding tPA activity (U/mL).

**Effects of intact or nicked  $\beta_2$ -GPI on tPA activity: fibrin plate assay.** To exclude the possibility that nicked  $\beta_2$ -GPI affected S-2251 cleavage without interacting with fibrinolytic factors, fibrinolysis was evaluated by conventional fibrin plate assays. Fibrin was layered on a plastic plate 10 cm in diameter, using the same volumes of 0.2% plasminogen-free fibrin (Sigma Chemical), 1% agarose, and 200  $\mu$ L/plate thrombin, 20 U/mL. Then, 6  $\mu$ L of the diluted tPA solution ("Effects of intact or nicked  $\beta_2$ -GPI on tPA activity: chromogenic assay") was incubated with the same volume of Glu-plasminogen (70  $\mu$ g/mL) in assay buffer, with intact or nicked  $\beta_2$ -GPI (up to 0.5  $\mu$ M). After 36 hours of incubation at 37°C, the area of lysis rings was measured. A standard curve was generated from serial dilutions of tPA.

**Statistical analysis.** Statistical evaluation was performed by the *t* test, Fisher exact test,  $\chi^2$  test, or Spearman rank correlation as appropriate. *P* values less than .05 were considered statistically significant.

## Results

### Levels of nicked $\beta_2$ -GPI in plasma samples

The plasma levels of nicked  $\beta_2$ -GPI ratio are shown in Figure 1. A normal level of nicked  $\beta_2$ -GPI ratio was derived from the apparently healthy subjects without any MRI abnormality, the mean plus 1 SD representing the upper limit of normal. A higher prevalence of elevated nicked  $\beta_2$ -GPI ratio was found in patients with ischemic stroke (63%, 39 of 62) and healthy subjects with lacunar infarct (27%, 14 of 52) when compared to healthy subjects with normal MRI findings (8%, 6 of 78). Relative risks of having stroke or asymptomatic lacunar infarction were approximated by odds ratio (95% CI), 20.3 (7.6-54.2) and 4.4 (1.6-12.4), respectively.

The prevalence of elevated levels of markers of thrombin generation and fibrinolytic turnover in our population are shown in Figure 2. A statistically significant correlation was observed between levels of PPI and nicked  $\beta_2$ -GPI ratio in plasma of healthy subjects with lacunar infarct ( $r^2 = 0.31$ ,  $P = .02$ ). No correlations were found between nicked  $\beta_2$ -GPI ratio and DDs or TAT complexes in any of the groups.

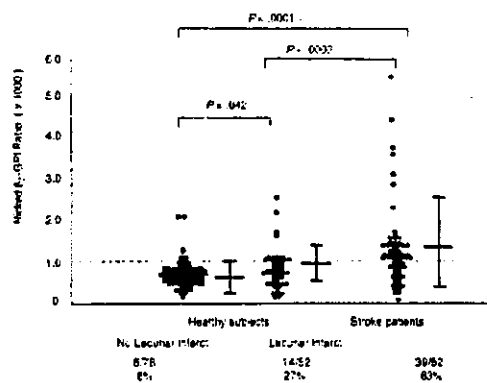


Figure 1. Plasma levels of nicked  $\beta_2$ -GPI. Total and nicked  $\beta_2$ -GPI plasma levels were determined by ELISA. A nicked  $\beta_2$ -GPI ratio, (plasma nicked  $\beta_2$ -GPI/plasma total  $\beta_2$ -GPI)  $\geq 1000$ , was established in all the samples. The dashed line indicates the mean + 1 SD of the ratio in healthy subjects without lacunar infarct. *P* values were calculated using *t* test.

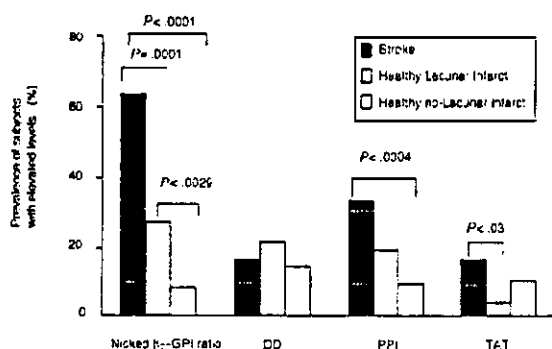


Figure 2. Prevalence of abnormally elevated plasma levels of nicked  $\beta_2$ -GPI and of markers of thrombin generation/fibrinolytic turnover in our population. Plasma levels of D-dimers (DD), plasmin-antiplasmin complex (PPI), and thrombin-antithrombin complexes (TAT) were determined in all the subjects as described in "Patients, materials, and methods."

In the apparently healthy subjects group ( $n = 130$ ), plasma nicked  $\beta_2$ -GPI ratio significantly correlated with age ( $r^2 = 0.483$ ,  $P < .0001$ ; Figure 3). Therefore, plasma measurement of nicked  $\beta_2$ -GPI might be a useful screening tool in the assessment of patients at risk of ischemic stroke.

#### Binding of nicked $\beta_2$ -GPI to Glu-plasminogen

The binding of up to  $0.4 \mu\text{M}$  nicked  $\beta_2$ -GPI to solid-phase Glu-plasminogen occurred in a dose-dependent manner, whereas the same concentrations of intact  $\beta_2$ -GPI did not bind to Glu-plasminogen (Figure 4A). The binding of Cof-22 to  $\beta_2$ -GPI was not affected by the cleavage of  $\beta_2$ -GPI. Molecular interaction between intact or nicked  $\beta_2$ -GPI and plasminogen was investigated using an optical biosensor. Nicked  $\beta_2$ -GPI showed a large extent of binding to immobilized Glu-plasminogen, whereas intact  $\beta_2$ -GPI did not show any specific binding (Figure 4B). The data of  $k_{\text{on}}$  at different concentrations of nicked  $\beta_2$ -GPI were fitted using linear regression, determining  $k_{\text{on}}$  as  $0.0006 \text{ M}^{-1}\text{s}^{-1}$  and  $k_{\text{off}}$  as  $0.0022 \text{ s}^{-1}$  (Figure 4C). Accordingly,  $K_D$  and  $K_A$  were determined as  $0.37 \times 10^{-6} \text{ M}$  and  $2.70 \times 10^6 \text{ M}^{-1}$ , respectively.

#### Inhibition of binding of Glu-plasminogen to nicked $\beta_2$ -GPI by the fragments of plasminogen or by EACA

The binding of Glu-plasminogen ( $10 \mu\text{g/mL}$ ) to immobilized nicked  $\beta_2$ -GPI, but not to native  $\beta_2$ -GPI, was demonstrated by ELISA. For the inhibition assay, the fragments of plasminogen (mini-plasminogen or kringle 4) as the inhibiting factors were added to the wells coated with nicked  $\beta_2$ -GPI, and bound Glu-plasminogen was detected using a monoclonal antikringle 1 to 3 antibody. Mini-plasminogen, but not kringle 4, inhibited the binding between Glu-plasminogen and nicked  $\beta_2$ -GPI (Figure 5A). Kringle 1 to 3 fragment or mini-plasminogen was added as inhibitor and bound Glu-plasminogen was detected using a monoclonal antikringle 4 antibody. Glu-plasminogen binding to nicked  $\beta_2$ -GPI was dose dependently inhibited by mini-plasminogen but not by kringle 1 to 3 fragment (Figure 5B). The fifth domain or the catalytic domain of Glu-plasminogen, therefore, was predicted to mediate its binding to nicked  $\beta_2$ -GPI.

When the binding of nicked  $\beta_2$ -GPI ( $10 \mu\text{g/mL}$ ) to solid-phase Glu-plasminogen was tested in the presence of different concentrations of EACA, the binding between nicked  $\beta_2$ -GPI and immobilized Glu-plasminogen was abolished in a dose-dependent manner (Figure 5C). Accordingly, LBS on plasminogen might mediate the binding of nicked  $\beta_2$ -GPI to Glu-plasminogen.

#### Binding of plasminogen to fibrin interfered with by nicked $\beta_2$ -GPI

We also investigated whether nicked  $\beta_2$ -GPI has an effect on the binding of Glu-plasminogen to immobilized fibrin monomer using an ELISA system. After preincubation with nicked  $\beta_2$ -GPI, but not with intact  $\beta_2$ -GPI, Glu-plasminogen showed decreased binding activity to soluble fibrin monomer (Figure 5D).

#### Effects of nicked $\beta_2$ -GPI on extrinsic fibrinolysis

The amidolytic activity of newly generated plasmin was evaluated as tPA activity (U/mL) in a chromogenic assay. The activity increased with the concentration of tPA (data not shown). When nicked  $\beta_2$ -GPI was added, the tPA activity decreased in a dose-dependent manner (Figure 6A). Intact  $\beta_2$ -GPI at  $0.25 \mu\text{M}$  did not suppress the fibrinolytic activity, whereas intact  $\beta_2$ -GPI in a higher concentration ( $0.50 \mu\text{M}$ ) slightly suppressed the fibrinolytic activity. The same amount of BSA or the recombinant domain I to IV of  $\beta_2$ -GPI did not affect the tPA activity.

The fibrinolytic activity of generated plasmin was measured as tPA activity (U/mL) in a fibrin plate assay. Fibrinolytic activity was suppressed by nicked  $\beta_2$ -GPI at  $0.25$  and  $0.50 \mu\text{M}$ . Intact  $\beta_2$ -GPI at  $0.50 \mu\text{M}$  also slightly inhibited the fibrinolytic activity. However,  $0.25 \mu\text{M}$  intact  $\beta_2$ -GPI did not affect the fibrinolytic activity of tPA (Figure 6B).

## Discussion

In the first part of this study, we demonstrated that plasma levels of nicked  $\beta_2$ -GPI were elevated in patients with ischemic stroke, indicating an elevated degree of fibrin turnover, but lower than that of DIC where thrombin and plasmin are massively generated.

In fact, nicked  $\beta_2$ -GPI was detected in large quantities in plasma of patients with DIC, a pathologic state characterized by marked increase of plasma PPI.<sup>22</sup> We observed a strong correlation between plasma levels of nicked  $\beta_2$ -GPI and those of PPI in the healthy individuals showing lacunar infarcts on MRI, suggesting that nicked  $\beta_2$ -GPI may rather reflect "minor" plasmin generation. In the presence of larger plasmin generation, the correlation between nicked  $\beta_2$ -GPI and PPI may be lost,<sup>23</sup> presumably due to the consumption of  $\alpha_2$ -AP. In individuals with MRI abnormalities the prevalence of increased nicked  $\beta_2$ -GPI ratio was higher than that of PPI, DDs, and TAT complexes (46%, 27%, 19%, and 11%, respectively). Thus, the detection of nicked  $\beta_2$ -GPI may

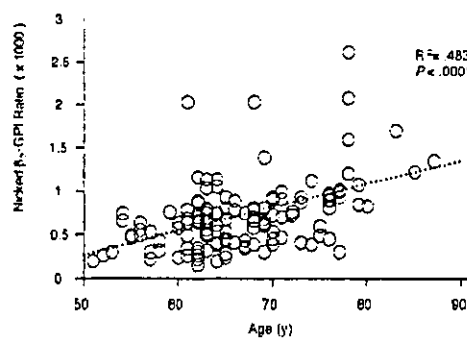
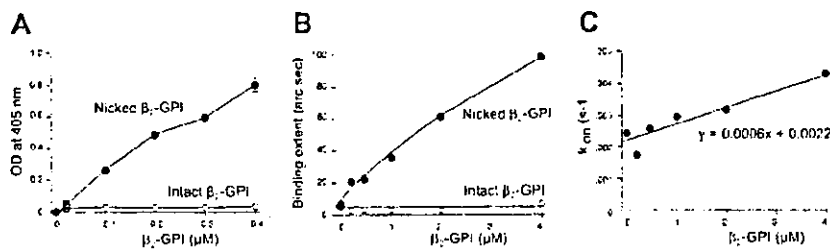


Figure 3. Correlation between plasma levels of nicked  $\beta_2$ -GPI and age in apparently healthy subjects. Nicked  $\beta_2$ -GPI was measured by a sandwich ELISA. The dotted line represents the regression curve. Each circle shows nicked  $\beta_2$ -GPI ratio and age in each subject.



**Figure 4. Binding of intact/nicked  $\beta_2$ -GPI to Glu-plasminogen.** (A) Binding of intact or nicked  $\beta_2$ -GPI to immobilized Glu-plasminogen was evaluated by ELISA using mouse monoclonal anti- $\beta_2$ -GPI antibody Cof-22. Closed circles indicate the dose-dependent binding of nicked  $\beta_2$ -GPI to Glu-plasminogen, whereas open circles indicate that intact  $\beta_2$ -GPI is unable to bind to Glu-plasminogen. (B-C) Kinetic plot showing molecular interaction between Glu-plasminogen and intact or nicked  $\beta_2$ -GPI. Intact  $\beta_2$ -GPI or nicked  $\beta_2$ -GPI binding to Glu-plasminogen was detected using IAsys, an optical biosensor as described in "Patients, materials, and methods." Binding extent (arc sec) was compared between intact and nicked  $\beta_2$ -GPI (B). Obtained on-rate constant ( $k_{on}$ ) for nicked  $\beta_2$ -GPI was plotted and fitted using linear regression to find the intercept and gradient (C). A formula for determining the association rate constant ( $k_{ass}$ ) and dissociation rate constant ( $k_{dis}$ ) is as follows:  $k_{on} = k_{diss} + k_{ass} [\text{ligand}]$ . Error bars indicate SDs.

represent a more sensitive marker of vascular lesions than PPI, DDs, or TAT complexes.

In support of this concept is the correlation between nicked  $\beta_2$ -GPI ratio and age in the apparently healthy subjects, suggesting that "minor" plasmin generation might be associated with subclinical or early clinical atherosclerosis. It is widely accepted that atherosclerosis is associated with endothelial cell activation and minor plaque rupture leading to small thrombus formation, secretion of t-PA, and plasmin generation, ultimately cleaving  $\beta_2$ -GPI. Indeed, nicked  $\beta_2$ -GPI can be generated on the surface of activated endothelial cells or platelets.<sup>23</sup>

In the second part of this study, we investigated the properties of nicked  $\beta_2$ -GPI in vitro to evaluate the biologic significance of our observations. We showed that nicked  $\beta_2$ -GPI specifically binds to Glu-plasminogen and inhibits extrinsic fibrinolysis in vitro. In contrast, neither domain I to IV of  $\beta_2$ -GPI nor intact  $\beta_2$ -GPI revealed such functions. The administration of intact  $\beta_2$ -GPI in higher concentrations also suppressed plasmin generation, perhaps owing to the nicked  $\beta_2$ -GPI produced by the newly generated plasmin. Under clinical conditions characterized by massive plasmin generation such as DIC or acute thrombosis, plasmin is generated by tPA released from activated endothelial cells with thrombus formation, and plasmin cleaves  $\beta_2$ -GPI on the thrombus, changing the properties of  $\beta_2$ -GPI. We propose that  $\beta_2$ -GPI is a precursor of plasmin-nicked  $\beta_2$ -GPI, a physiologic inhibitor of fibrinolysis.

The crystal structure of human  $\beta_2$ -GPI has been defined.<sup>28,29</sup> Bouma et al<sup>28</sup> proposed that a large positively charged patch in domain V binds to anionic surfaces with a flexible and partially

hydrophobic loop inserted into the lipid layer. According to the conformation of the nicked domain V, as predicted from the x-ray structure of the intact domain V and confirmed by heteronuclear magnetic resonance, the nicked C-terminal loop is tightly fixed by electrostatic interaction with enhanced stability, the result being neutralization of the positive charge of the lysine cluster.<sup>26,30</sup>

Glu-plasminogen, a full-length protein, is the naturally circulating form of plasminogen. Kringle 5 of Glu-plasminogen has a higher affinity for intact fibrin.<sup>31,32</sup> LBS in kringle 5 of Glu-plasminogen mediates its binding to N-terminal lysine on fibrin, an event essential to initiate fibrinolysis reactions. This initial binding of Glu-plasminogen to fibrin induces a conformational change from a "closed" to an "open" form, thus promoting accessibility to plasminogen activators such as tPA or urokinase.<sup>19</sup> On the fibrin surface, generated plasmin cleaves the single-chain tPA into the 2-chain tPA, a more active form, providing a positive feedback for plasmin generation. Plasmin simultaneously degrades fibrin and makes C-terminal lysine of fibrin more accessible to plasminogen via kringles 1,<sup>33,34</sup> 2, and 3,<sup>35</sup> thus accelerating fibrinolysis.

According to the results of the inhibition studies using plasminogen fragments or EACA (Figure 5), and comparison of the effect on plasmin generation between nicked  $\beta_2$ -GPI and domain I to IV of  $\beta_2$ -GPI (Figure 6A), it would be indicated that the binding of nicked  $\beta_2$ -GPI to Glu-plasminogen is mediated by the interaction between the lysine-cluster patch in domain V of the nicked  $\beta_2$ -GPI and LBS on the plasminogen kringle 5,<sup>36</sup> although it still may be possible that an excess amount of EACA interacts with the catalytic domain of Glu-plasminogen. The conformational difference between intact and nicked  $\beta_2$ -GPI is critical for its binding to

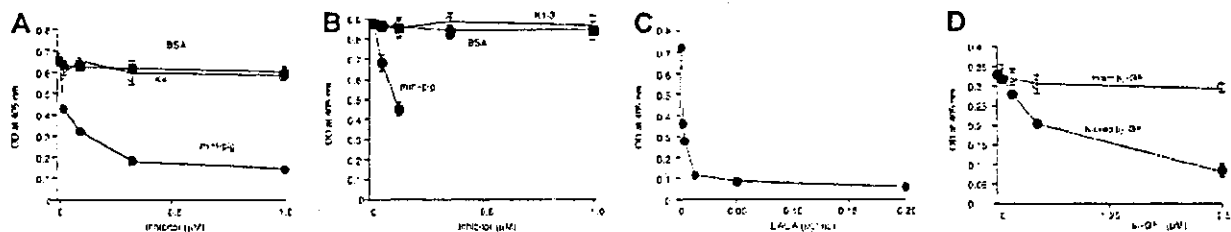


**Figure 5. Identification of the binding site of Glu-plasminogen to  $\beta_2$ -GPI by inhibition ELISA using plasminogen fragments.** (A) Binding of Glu-plasminogen to immobilized nicked  $\beta_2$ -GPI was tested by ELISA in the presence of possible inhibitors. After nicked  $\beta_2$ -GPI immobilization onto microtiter plates, different concentrations of kringle 4 of plasminogen (□) or mini-plasminogen (that consists of kringle 5 and catalytic domain of plasminogen; ●) were added as inhibitors. BSA (■) served as control. After incubation and washing, Glu-plasminogen (10  $\mu$ g/mL) was added and bound Glu-plasminogen was determined using kringle 1- to 3-specific mouse monoclonal antiplasminogen antibody. (B) For the inhibition ELISA kringle 1 to 3 of plasminogen (□) or mini-plasminogen (●) served as inhibitors. Glu-plasminogen bound to immobilized  $\beta_2$ -GPI was detected using kringle 4-specific mouse monoclonal antiplasminogen antibody. Assays were run in triplicate. (C) Competitive ELISA using EACA, a lysine homologue. Binding of nicked  $\beta_2$ -GPI (0.2  $\mu$ M) to immobilized Glu-plasminogen was tested by ELISA using Cof-22 antibody in the presence of various concentrations of EACA (0-0.20  $\mu$ g/mL). (D) Soluble fibrin monomer (5  $\mu$ g/mL) was coated on the surface of a microtiter plate and blocked. Biotinylated Glu-plasminogen (5  $\mu$ g/mL) was preincubated with intact or nicked  $\beta_2$ -GPI and added to the wells. After incubation and washing, ALP-conjugated streptavidin was used for detection. Assays were run triplicate. Error bars indicate SDs. K indicates kringle; mini-plg, mini-plasminogen.

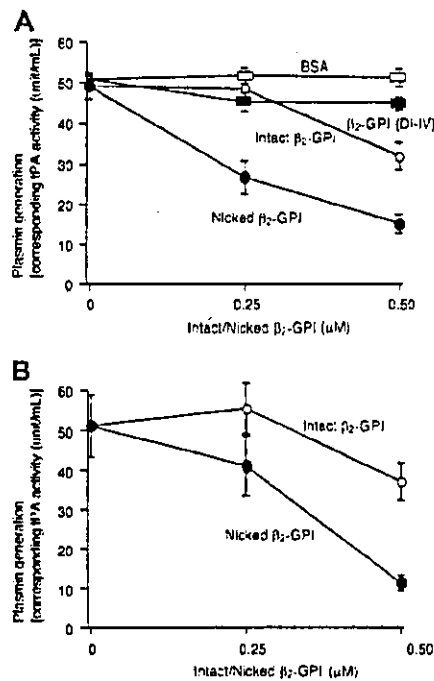


**Figure 6.** Inhibitory effect of nicked  $\beta_2$ -GPI on plasmin generation. (A) Plasmin generation was measured by parabolic rate assay using synthetic substrate S-2251 in the presence of tPA, Glu-plasminogen, and fibrin monomer. Nicked  $\beta_2$ -GPI ( $\bullet$ ), intact  $\beta_2$ -GPI ( $\circ$ ),  $\beta_2$ -GPI domain I-IV mutant ( $\blacksquare$ ), or BSA ( $\square$ ) was added to the reaction in the indicated concentrations. After 12 hours of incubation, absorbance at 405 nm was measured and expressed as tPA activity (U/mL) using tPA as standard. (B) Fibrinolytic activity was measured using fibrin plate assay. Solution reaction containing tPA, Glu-plasminogen, and nicked ( $\bullet$ ) or intact  $\beta_2$ -GPI ( $\circ$ ) were placed onto fibrin plates. After 36 hours of incubation, the ring area of lysis was measured. Assays were performed in triplicate. Error bars indicate SDs. D indicates domain.

phospholipid or plasminogen. The lysine-cluster patch in domain V of nicked  $\beta_2$ -GPI may gain accessibility for the LBS of Glu-plasminogen, whereas the C-terminal loop of intact  $\beta_2$ -GPI may

interfere with interactions of LBS and the Glu-plasminogen kringle 5.

The fibrinolytic system is regulated at different levels, either at plasminogen activation or at enzymatically active plasmin. Many factors, including  $\alpha_2$ -AP,  $\alpha_2$ -macroglobulin,  $\alpha_1$ -antitrypsin, inactivated C1, PAI-1, and PAI-2, prevent the overactivation of the fibrinolytic system. The most potent inhibitors are  $\alpha_2$ -AP and PAI-1<sup>37</sup>; the former binds to a component of kringle 1 to 3 of plasminogen<sup>38</sup> and can neutralize the generated plasmin more rapidly than  $\alpha_2$ -macroglobulin.

Fibrinolysis initiates on binding of kringle 5 of plasminogen to lysine residues on lysine followed by the binding of kringle 1 to 3 of plasminogen to lysine residues on the cleaved fibrin.  $\alpha_2$ -AP does not bind to kringle 5 of plasminogen, hence, does not seem to affect the first interaction. Based on the observation that nicked  $\beta_2$ -GPI interferes the binding between Glu-plasminogen and fibrin monomer (Figure 5D), it is likely that the binding of nicked  $\beta_2$ -GPI to Glu-plasminogen affects the first step of fibrinolysis at least and exerts an inhibitory function in the fibrinolytic system via different mechanisms from that of  $\alpha_2$ -AP.

In conclusion, first we have demonstrated that plasma levels of nicked  $\beta_2$ -GPI can be a sensitive marker of cerebral ischemic events and we suggest that plasma measurement of nicked  $\beta_2$ -GPI might be a useful screening tool in the assessment of patients at risk of ischemic stroke. Second, we propose that nicked  $\beta_2$ -GPI is a physiologic inhibitor of fibrinolysis and that plasmin cleavage of  $\beta_2$ -GPI is part of the negative feedback pathway of extrinsic fibrinolysis.

## Acknowledgment

We wish to thank Professor Koji Suzuki, from Department of Molecular Pathobiology, Mie University School of Medicine, Tsu, Japan, for great suggestions and fruitful discussions.

## References

- Galli M, Comfurius P, Maessen C, et al. Anticardiolipin antibodies (ACA) directed not to cardiolipin but to a plasma protein cofactor. *Lancet*. 1990;335:1544-1547.
- McNeil HP, Simpson RJ, Chesterman CN, Krilis SA. Anti-phospholipid antibodies are directed against a complex antigen that induces a lipid-binding inhibitor of coagulation:  $\beta_2$ -glycoprotein I (apolipoprotein H). *Proc Natl Acad Sci U S A*. 1990;87:4120-4124.
- Matsuura E, Igarashi Y, Fujimoto M, Ichikawa K, Koike T. Anticardiolipin cofactor(s) and differential diagnosis of autoimmune disease. *Lancet*. 1990;336:177-178.
- Hughes GRV. The antiphospholipid syndrome: ten years on. *Lancet*. 1993;342:341-344.
- Hunt JE, Simpson RJ, Krilis SA. Identification of a region of  $\beta_2$ -glycoprotein I critical for lipid binding and anti-cardiolipin antibody cofactor activity. *Proc Natl Acad Sci U S A*. 1993;90:2141-2145.
- Ohkura N, Hagihara Y, Yoshimura T, Goto Y, Kato H. Plasmin can reduce the function of human  $\beta_2$  glycoprotein I by cleaving domain V into a nicked form. *Blood*. 1998;91:4173-4179.
- Nimpf J, Bevers EM, Bomans PHH, et al. Prothrombinase activity of human platelets inhibited by  $\beta_2$ -glycoprotein I. *Biochim Biophys Acta*. 1986;884:142-149.
- Shi W, Chong BH, Hogg PJ, Chesterman CN. Anticardiolipin antibodies block the inhibition by  $\beta_2$ -glycoprotein I of the factor Xa generating activity of platelets. *Thromb Haemost*. 1993;70:342-345.
- Schousboe I, Rasmussen MS. Synchronized inhibition of the phospholipid mediated autoactivation of factor XII in plasma by  $\beta_2$ -glycoprotein I and anti- $\beta_2$ -glycoprotein I. *Thromb Haemost*. 1995;73:798-804.
- Mori T, Takeya H, Nishioka J, Gabazza EC, Suzuki K.  $\beta_2$ -Glycoprotein I modulates the anticoagulant activity of activated protein C on the phospholipid surface. *Thromb Haemost*. 1996;75:49-55.
- Ieko M, Ichikawa K, Triplett DA, et al.  $\beta_2$ -Glycoprotein I is necessary to inhibit protein C activity by monoclonal anticardiolipin antibodies. *Arthritis Rheum*. 1999;42:167-174.
- Nakaya Y, Schaefer EJ, Brewer HBJ. Activation of human post heparin lipoprotein lipase by apolipoprotein H ( $\beta_2$ -glycoprotein I). *Biochim Biophys Res Commun*. 1980;95:1168-1172.
- Wurm H, Beubler E, Polz E, Holasek A, Kostner G. Studies on the possible function of  $\beta_2$ -glycoprotein-I: influence in the triglyceride metabolism in the rat. *Metabolism*. 1982;31:484-486.
- Hasunuma Y, Matsuura E, Makita Z, Kalahira T, Nishi S, Koike T. Involvement of  $\beta_2$ -glycoprotein I and anticardiolipin antibodies in oxidatively modified low-density lipoprotein uptake by macrophages. *Clin Exp Immunol*. 1997;107:569-573.
- Chonn A, Semple SC, Cullis PR.  $\beta_2$  glycoprotein I is a major protein associated with very rapidly cleared liposomes in vivo, suggesting a significant role in the immune clearance of "non-self" particles. *J Biol Chem*. 1995;270:25845-25849.
- Manfredi AA, Rovere P, Galati G, et al. Apoptotic cell clearance in systemic lupus erythematosus; I: opsonization by antiphospholipid antibodies. *Arthritis Rheum*. 1998;41:205-214.
- Manfredi AA, Rovere P, Heltai S, et al. Apoptotic cell clearance in systemic lupus erythematosus; II: role of  $\beta_2$ -glycoprotein I. *Arthritis Rheum*. 1998;41:215-223.
- Wallen P, Wiman B. Characterization of human plasminogen; I: on the relationship between different molecular forms of plasminogen demonstrated in plasma and found in purified preparations. *Biochim Biophys Acta*. 1970;221:20-30.
- Ponting CP, Holland SK, Cederholm-Williams SA, et al. The compact domain conformation of human Glu-plasminogen in solution. *Biochim Biophys Acta*. 1992;1159:155-161.
- Aoki N, Saito H, Kamiya T, Koie K, Sakata Y, Kobakura M. Congenital deficiency of  $\alpha_2$ -plasmin inhibitor associated with severe hemorrhagic tendency. *J Clin Invest*. 1979;63:877-884.
- Loskutoff DJ, Sawdey M, Mimuro J. Type 1 plasminogen activator inhibitor. *Prog Hemost Thromb*. 1989;9:87-115.
- Horbach DA, van Oort ET, Lisman T, Meijers JC,

- Derksen RH, de Groot PG.  $\beta$ 2-Glycoprotein I is proteolytically cleaved *in vivo* upon activation of fibrinolysis. *Thromb Haemost*. 1999;81:87-95.
23. Itoh Y, Inuzuka K, Kohno I, et al. Highly increased plasma concentrations of the nicked form of  $\beta$ 2-glycoprotein I in patients with leukemia and with lupus anticoagulant: measurement with a monoclonal antibody specific for a nicked form of domain V. *J Biochem (Tokyo)*. 2000;128:1017-1024.
  24. Igarashi M, Matsuura E, Igarashi Y, et al. Human  $\beta$ 2-glycoprotein I as an anticardiolipin cofactor determined using deleted mutants expressed by a Baculovirus system. *Blood*. 1996;87:3262-3270.
  25. Matsuura E, Igarashi Y, Fujimoto M, et al. Heterogeneity of anticardiolipin antibodies defined by the anticardiolipin cofactor. *J Immunol*. 1992;148:3885-3891.
  26. Matsuura E, Inagaki J, Kasahara H, et al. Proteolytic cleavage of  $\beta$ 2-glycoprotein I: reduction of antigenicity and the structural relationship. *Int Immunol*. 2000;12:1183-1192.
  27. Ranby M, Wallen P. A sensitive parabolic rate assay for tissue plasminogen activator. In: Davidson JF, Nilson LM, Asted B, eds. *Progress in Fibrinolysis*. Vol 5. New York, NY: Churchill Livingstone; 1981:232-235.
  28. Bouma B, de Groot PG, van den Elsen JM, et al. Adhesion mechanism of human  $\beta$ 2-glycoprotein I to phospholipids based on its crystal structure. *EMBO J*. 1999;18:5166-5174.
  29. Schwarzenbacher R, Zeth K, Diederichs K, et al. Crystal structure of human  $\beta$ 2-glycoprotein I: implications for phospholipid binding and the antiphospholipid syndrome. *EMBO J*. 1999;18:6228-6239.
  30. Hoshino M, Hagihara Y, Nishii I, Yamazaki T, Kato H, Goto Y. Identification of the phospholipid-binding site of human  $\beta$ 2-glycoprotein I domain V by heteronuclear magnetic resonance. *J Mol Biol*. 2000;304:927-939.
  31. Lucas MA, Fretto LJ, McKee PA. The binding of human plasminogen to fibrin and fibrinogen. *J Biol Chem*. 1983;258:4249-4256.
  32. Wu HL, Chang BI, Wu DH, et al. Interaction of plasminogen and fibrin in plasminogen activation. *J Biol Chem*. 1990;265:19658-19664.
  33. Christensen U. C-terminal lysine residues of fibrinogen fragments essential for binding to plasminogen. *FEBS Lett*. 1985;182:43-46.
  34. Tran-Thang C, Kruihof EK, Atkinson J, Bachmann F. High-affinity binding sites for human Glu-plasminogen unveiled by limited plasminic degradation of human fibrin. *Eur J Biochem*. 1986;160:599-604.
  35. Matsuka YV, Novokhatny VV, Kudinov SA. Fluorescence spectroscopic analysis of ligand binding to kringle 1 + 2 + 3 and kringle 1 fragments from human plasminogen. *Eur J Biochem*. 1990;190:93-97.
  36. Chang Y, Mochalkin I, McCance SG, Cheng B, Tulinsky A, Castellino FJ. Structure and ligand binding determinants of the recombinant kringle 5 domain of human plasminogen. *Biochemistry*. 1998;37:3258-3271.
  37. Collen D, Lijnen HR. Basic and clinical aspects of fibrinolysis and thrombolysis. *Blood*. 1991;78:3114-3124.
  38. Thorsen S, Clemmensen I, Sottrup-Jensen L, Magnusson S. Adsorption to fibrin of native fragments of known primary structure from human plasminogen. *Biochem Biophys Acta*. 1981;668:377-387.

## Alternate Promoter and 5'-Untranslated Exon Usage of the Mouse Adrenocorticotropin Receptor Gene in Adipose Tissue

MITSUMASA KUBO, CHIKARA SHIMIZU\*, HIROMICHI KIJIMA\*, SOH NAGAI\* AND TAKAO KOIKE\*

Health Administration Center, Hokkaido University of Education, 5-3-1 Ainosato, Kita-ku, Sapporo 002-8501, Japan

\*Department of Medicine II, Hokkaido University School of Medicine, N-15, W-7, Kita-ku, Sapporo 060-8638, Japan

**Abstract.** Mouse adrenocorticotropin receptor (ACTH-R/MC2R) messenger ribonucleic acid (mRNA) is expressed predominantly in the adrenal gland and, to a lesser extent, in adipose tissue. In this study, we found a novel 135-bp exon 1 (exon 1f) of the ACTH-R gene transcribed in mouse adipose tissue by RNA ligase-mediated rapid amplification of cDNA ends, which was located 1.4 kb downstream in the genome of previously-reported exon 1 (exon 1a) transcribed in the adrenal gland. The novel promoter region, 1.4 kb upstream of exon 1f contained three CCAAT boxes. RT-PCR analysis revealed that ACTH-R mRNA from adipose tissue and differentiated 3T3-L1 adipocytes exclusively contained exon 1f. Thus, the promoter region flanking to exon 1f is thought to be essential for adipose tissue, while that flanking to exon 1a is specific for the adrenal gland. A search for a similar sequence of mouse ACTH-R exon 1f and its flanking region in the human genome sequence database of GenBank Human Genome Resources did not reveal such a sequence in the region of the human ACTH-R gene. This may explain the absence of ACTH-R expression in human adipose tissue.

**Key words:** ACTH receptor, Adipose tissue, Alternate promoter, Mouse

(Endocrine Journal 51: 25–30, 2004)

**THE** analysis of mouse adrenal cDNA and genomic DNA revealed that the adrenocorticotropin receptor (ACTH-R/MC2R) gene consists of four exons [1]: the first three exons encode the 5'-untranslated region (UTR) and the fourth exon encodes part of 5'-UTR, the entire coding region, and the whole of 3'-UTR. Two mRNA species, one with and one without 57-bp exon 2 by alternative splicing were demonstrated in the adrenal gland [1]. The human ACTH-R gene consists of two constant exons and one alternate exon between them [2, 3]: the first exon and alternate exon encode 5'-UTR and the other encodes part of 5'-UTR, the entire coding region, and the whole of 3'-UTR. The coding region of the ACTH-R gene in both species shows an 84.6% nucleotide identity. The first exon and the proximal promoter region of the gene in

the two species are also well conserved. However, mouse exons 2 and 3 show no homology to any sequences of the human ACTH-R gene.

It is well known that ACTH does not act directly upon human adipose tissue [4, 5], but is bound to the membrane receptor specific for ACTH itself in rat adipose tissue [6] and stimulates intracellular cAMP production and lipolysis in adipose tissue of mouse, rabbit, and rat [7–9]. ACTH-R mRNA was demonstrated in adipose tissue of mouse but not of human [10]. To clarify the mechanism(s) of the different expression of the ACTH-R gene in adipose tissue of mouse and human, we performed RNA ligase-mediated rapid amplification of cDNA ends (RLM-RACE) [11, 12] using total RNA from mouse adipose tissue and found a novel 5'-UTR exon 1. The sequence in the human ACTH-R gene similar to that of novel exon 1 and its 5' flanking region (proximal promoter) of the mouse gene was not found when searched for in the human genome sequence database of GenBank Human Genome Resources.

Received: July 28, 2003

Accepted: September 9, 2003

Correspondence to: Mitsumasa KUBO, M.D., Health Administration Center, Hokkaido University of Education, 5-3-1 Ainosato, Kita-ku, Sapporo 002-8501, Japan

## Materials and Methods

### Oligonucleotide primers

Sequences of oligonucleotide primers were: mCTR1AS (antisense; coding region; 464–481 of GenBank accession number NM\_008560), 5'-CAGACTGCCCAACATGTC; mCTR2AS (antisense; coding region; 988–1005 of NM\_008560), 5'-TAAGGGTTATTTGGGCAG; mCTRASN (antisense; coding region; 314–331 of NM\_008560), 5'-AACTACATCAGGACAATC; mCTREX1S (sense; shown in Fig. 2), 5'-CAGTCATCTTGCCGAGAAAG; mCTRalt1S (sense; shown in Fig. 2), 5'-CAAGGGA GGCAGAAACTG.

### Animals, cell culture, and RNA extraction

Std:ddY mice 8 weeks of age were obtained from Japan SLC Inc. Total RNA from adrenal glands and epididymal adipose tissue was extracted by cesium-chloride ultracentrifugation. Y-1 mouse adrenocortical cells were cultured in F-10 medium and 10% fetal calf serum (FCS). 3T3-L1 cells were grown in Dulbecco Modified Eagle's Medium (DMEM) and 10% FCS until confluent, followed by an enhancement of differentiation by an addition of 0.5 mM 1-methyl-3-isobutylxanthine, 0.25 mM dexamethasone, and insulin (1 mg/ml) for 2 days [13]. Cells were then fed in DMEM and 10% FCS and used within 5 to 7 days. Total RNA from cells was extracted by guanidinium thiocyanate-phenol-chloroform method.

### RNA ligase-mediated rapid amplification of cDNA ends

RLM-RACE was performed using FirstChoice RLM-RACE kit (Ambion, USA) according to manufacturer directions. In brief, 10 µg of total RNA from mouse epididymal adipose tissue was incubated with calf intestinal phosphatase (CIP) followed by phenol/chloroform extraction. CIP-treated RNA was incubated with tobacco acid pyrophosphatase (TAP) at 37°C for 1 h. A synthetic RNA adapter (supplied in kit) was ligated to CIP/TAP-treated RNA as well as CIP-treated/TAP-untreated RNA by T<sub>4</sub> RNA ligase at 37°C for 1 h. Then, ligated RNA was annealed with mCTR2AS at 65°C for 5 min and reverse transcribed with ThermoScript RT (Life Technologies, USA) at 55°C for 50 min, followed by incubation at 85°C for 5 min for termination of reverse transcription. PCR

between mCTR1AS and Outer ADP-primer (supplied in kit) using CIP/TAP-treated and CIP-treated/TAP-untreated single strand cDNA as a template was initiated at 95°C for 9 min for activation of AmpliTaq Gold (Perkin Elmer, USA) and then carried out for 35 cycles consisting of denaturation at 94°C for 30 sec, annealing at 60°C for 30 sec, and extension at 72°C for 45 sec. The PCR products were electrophoresed on a 2.5% agarose gel, and cloned directly onto TA cloning vector (Invitrogen, USA) and sequenced on both strands using M13 and M13 reverse primers by ABIPRISM sequencing system (Perkin Elmer, USA).

### RT-PCR analysis of alternate first exon

Total RNA from mouse adrenal glands, epididymal adipose tissue, Y-1 cells, and 3T3-L1 cells (undifferentiated/differentiated) was reverse transcribed using oligo-dT<sub>15</sub> as a primer by Superscript II reverse-transcriptase (Life Technologies, USA), followed by PCR between oligonucleotide primers of mCTRalt1S and mCTR1AS, or mCTRalt1S and mCTRASN. PCR between mCTRalt1S and mCTR1AS was initiated at 95°C for 9 min for activation of AmpliTaq Gold, and then carried out for 30 cycles consisting of denaturation at 94°C for 30 sec, annealing at 60°C for 30 sec, and extension at 72°C for 1 min. PCR conditions between mCTRalt1S and mCTRASN were the same except of 35 cycles and annealing temperature 58°C. The PCR products were analyzed in a 0.8% or 2.5% agarose gel.

## Results

By RLM-RACE, an approximately 600-bp DNA band was demonstrated in a lane of TAP-treated RNA, but no DNA fragments in a lane of TAP-untreated RNA (Fig. 1). After cloning of the RLM-RACE products and sequencing of the clones (67 clones were totally obtained), 64 clones contained a part of the ACTH-R coding sequence, the whole of exon 3 with/without exon 2, and novel 5'-untranslated sequence 5' flanking to exons 3 and/or 2, indicating that the newly-identified 5'-UTR seems to be a novel exon 1 (exon 1f) (described later). Of the 64 clones, the 5' end of the insert cDNA of 24 clones was adenine numbered as +1 in Fig. 2, and of 19 clones adenine at -11, and of 8 clones adenine at +13. The 5' end of the insert

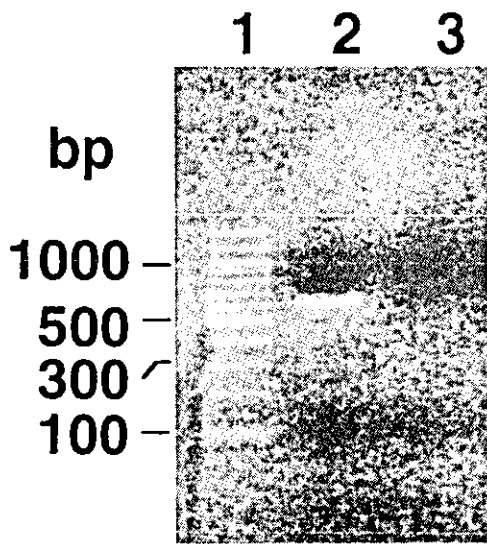


Fig. 1. Electrophoretic analysis of mouse adipose tissue cDNA obtained by RLM-RACE. Lane 1, 100 bp DNA ladder; lane 2, TAP-treated RNA; lane 3, TAP-untreated RNA.

cDNA of other clones was varied from -60 to +77. Sixteen clones of the 64 clones contained alternate exon 2. Of the 16 clones containing alternate exon 2, the 5' end of the insert cDNA of 8 clones was adenine at +1. Searching the novel exon 1f sequence in the genomic DNA insert of the  $\lambda$  phage clone containing exon 1 (designated exon 1a) expressed in the adrenal gland and isolated by our previous study [1], we found that exon 1f was located approximately 1.4 kb downstream of exon 1a.

To assure that exon 1f was expressed in adipose tissue, RT-PCR analysis was done. As shown in Fig. 3A, exon 1f was expressed in epididymal adipose tissue and adrenal glands (lanes 11 and 7), whereas exon 1a was demonstrated in adrenal glands but not in adipose tissue (lanes 1 and 5). Undifferentiated 3T3-L1 preadipocytes showed no ACTH-R cDNA (lanes 3 and 9). Differentiated 3T3-L1 adipocytes expressed only exon 1f (lanes 4 and 10), and Y-1 cells exclusively exon 1a

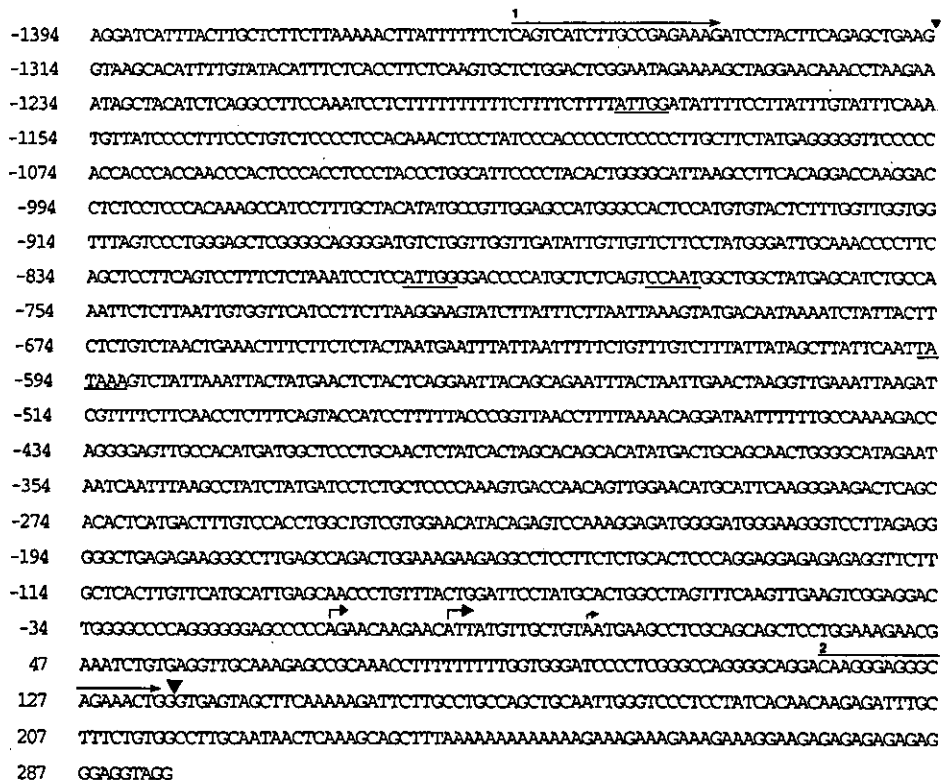
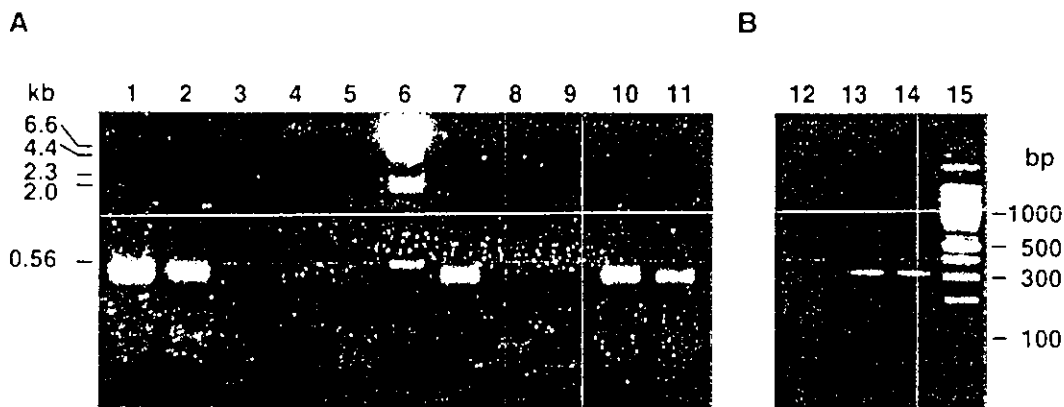


Fig. 2. Nucleotide sequence of the novel promoter region and exon 1f (see text) of the mouse ACTH-R gene. +1 corresponds to the possible major transcription start site as indicated by a large arrow. Two small arrows indicate possible minor transcription start sites. Large and small arrowheads denote the junction of exon 1f and intron sequence, and exon 1a and intron sequence, respectively. Three CCAAT boxes and a TATA box are underlined. The oligonucleotide primers, mCTREX1S and mCTRalt1S, are shown by line 1 and line 2 over the sequence, respectively. The sequence in the top (-1394 to -1315) is part of exon 1a.





**Fig. 3.** Electrophoretic analysis in 0.8% (panel A) and 2.5% (panel B) agarose gels of RT-PCR products using total RNA of mouse adrenals, epididymal adipose tissue, Y-1 cells, and undifferentiated/differentiated 3T3-L1 cells as a template. Primers for reverse transcription were oligo-dT<sub>15</sub>, and PCR was done between a set of primers, mCTREX1S and mCTR1AS for exon 1a (lane 1 to 5 in panel A), mCTRalt1S and mCTR1AS for exon 1f (lane 7 to 11 in panel A), and mCTRalt1S and mCTRASN for exon 1f (lane 12 to 14 in panel B). Lanes 1 and 7, adrenal glands; lanes 2 and 8, Y-1 cells; lanes 3, 9 and 12, undifferentiated 3T3-L1 preadipocytes; lanes 4, 10 and 13, differentiated 3T3-L1 adipocytes; lanes 5, 11 and 14, epididymal adipose tissue; lane 6,  $\lambda$  HindIII -digested DNA marker; lane 15, 100 bp DNA ladder.

(lanes 2 and 8).

In adipose tissue and differentiated 3T3-L1 adipocytes, RT-PCR between a set of primers, mCTRalt1S and mCTRASN demonstrated the predicted DNA fragments of 303 bp and 360 bp, and the latter contained 57-bp alternate exon 2 and was less prominent than the former (Fig. 3B, lanes 13 and 14).

### Discussion

In this study we found novel 5'-untranslated exon 1f (exon 1f) of the mouse ACTH-R gene transcribed in adipose tissue. RT-PCR analysis confirmed that mRNA from adipose tissue and differentiated 3T3-L1 adipocyte contained exon 1f, but no previously-proven exon 1a which was transcribed in the adrenal gland (Fig. 3A). Thus, exon 1f is unique for adipose tissue, and exon 1a specific for the adrenal gland. RT-PCR study also defined that mRNA from the adrenal gland contained exons 1a and 1f, independently, whereas mRNA from Y-1 mouse adrenocortical cells contained only exon 1a (Fig. 3A, lanes 1, 2, 7 and 8). It is conceivable that the presence of exon 1f transcripts in the adrenal gland was likely due to the contamination of periadrenal fat tissues while removing adrenal glands *in vivo*. Further investigation is required to ascertain whether or not exon 1f could be transcribed in the adrenal gland.

In the RLM-RACE study, we used CIP-treated and TAP-treated RNA to which a synthetic RNA adaptor was ligated. CIP treatment removed free 5' phosphates from degraded RNA, and following TAP treatment removed the cap structure from full-length mRNA, leaving a 5' monophosphate. Therefore, the RNA adaptor was ligated exclusively to full-length mRNA. As more than one third (24 clones) of 64 clones obtained by RLM-RACE contained 135-bp novel exon 1f sequence, the 5' end was thought to be a major transcription start site (numbered +1 in Fig. 1). Furthermore, while 19 clones contained 146-bp exon 1f sequence and 8 clones 122-bp exon 1f, those 5' ends were then deemed to be minor start sites. One-fourth (16 clones) of the 64 clones possessed 57-bp exon 2 which was alternatively spliced in the adrenal gland [1], and RT-PCR analysis revealed that mRNA from adipose tissue and 3T3-L1 adipocytes consisted of two mRNA populations, one with and one without exon 2, the latter being more prominent.

Analysis of the insert DNA fragment of the  $\lambda$  phage clone containing exon 1a previously isolated from mouse genomic DNA library [1] revealed that exon 1f was located approximately 1.4 kb downstream of exon 1a, and later this was confirmed when the exon 1f sequence in the mouse genome sequence database of GeneBank (accession number NT\_039674.1) was found. It was reported that the proximal promoter region flanking to exon 1a contained one SF-1 (steroido-

## Chromosome 18 37.0cM

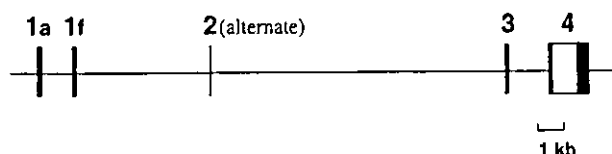


Fig. 4. Organization of the mouse ACTH-R gene. Coding region is a white box, and untranslated regions are black boxes.

genic factor 1) binding site lacking CCAAT boxes, a TATA box, and consensus CRE (cyclic AMP responsive element) sequence, and that SF-1 was essential for the promoter function in Y-1 cells [14]. The relevant promoter region of the human ACTH-R gene also contained a few SF-1 binding sites which were critical for the promoter activity in Y-1 cells, and several CRE-like sequences yet functionally undetermined, lacking CCAAT and TATA boxes [15, 16]. The 1.4 kb promoter region flanking to exon 1f contained three CCAAT boxes and a TATA box which was located approximately 600-bp upstream of the possible major transcription start site. There exist no consensus binding sites for CRE-binding protein, AP-1 (activating protein 1), SF-1, and PPAR $\gamma$  (peroxisome proliferator-activated receptor  $\gamma$ ). While expression of CCAAT/enhancer binding protein  $\alpha$  and PPAR $\gamma$  is known to occur during differentiation of 3T3-L1 preadipocytes and to be sustained in adipocytes [17], it is plausible that any CCAAT box(es) might be

responsible for ACTH-R gene expression in adipose tissue. However, the functional analysis of the newly-identified promoter region flanking to exon 1f is required to understand the precise regulation of ACTH-R gene expression in adipose tissue.

Exon 1a and the coding region of the ACTH-R gene in mouse and human have a high degree of sequence homology. A similar sequence of exon 1f and its surrounding region in the human genome sequence database of GenBank Human Genome Resources has been searched, but no such sequence in the region of the human ACTH-R gene has been found. This may explain the absence of ACTH-R mRNA in human adipose tissue.

The organization of the mouse ACTH-R gene, as determined by this study and previous reports along with the genome sequence data of GenBank Mouse Genome Resources, is depicted in Fig. 4. The gene spans approximately 23 kb on chromosome 18, 37.0 cM locus [18] and consists of exons 1a (195-bp) [14], 1f (135-bp), 2 (57-bp), 3 (112-bp), and 4 (1,477-bp). The distance between exons 1a and 1f, exons 1f and 2, exons 2 and 3, and exons 3 and 4 (coding exon) of the gene is 1,314 bp, 5,590 bp, 12,196 bp, and 1,490 bp, respectively.

### Acknowledgements

We thank Miki Ishida for excellent technical assistance.

### References

1. Shimizu C, Kubo M, Saeki T, Matsumura T, Ishizuka T, Kijima H, Kakinuma M, Koike T (1997) Genomic organization of the mouse adrenocorticotropin receptor. *Gene* 188: 17–21.
2. Naville D, Barihoux L, Jaillard C, Lebrethon MC, Saez JM, Begeot M (1994) Characterization of the transcription start site of the ACTH receptor gene: presence of an intronic sequence in the 5'-flanking region. *Mol Cell Endocrinol* 106: 131–135.
3. Kubo M, Shimizu C, Kijima H, Ishizuka T, Takano K, Takano A, Koike T (2000) Alternate exon in the 5'-untranslated region of the human ACTH receptor gene. *Endocr J* 47: 543–548.
4. Galton DJ, Bray GA (1967) Studies on lipolysis in human adipose cells. *J Clin Invest* 46: 621–629.
5. Poupon R (1975) Activity of human adenylate cyclase from human fat cell membranes. *Biomedicine* 23: 438–442.
6. Oelofsen W, Ramachandran J (1983) Studies of corticotropin receptors on rat adipocytes. *Arch Biochem Biophys* 225: 414–421.
7. Fan CC, Ho RJ (1981) Response of white adipocyte of mouse and rabbit to catecholamines and ACTH. 1. Correlation of cyclic AMP levels and initial rates of lipolysis. *Mol Cell Biochem* 34: 35–41.
8. White JE, Engel FL (1958) Lipolytic action of corticotropin on rat adipose tissue in vitro. *J Clin Invest* 37: 1556–1563.
9. Birnbaumer L, Pohl SL, Rodbell M (1969) Adenylate cyclase in fat cells. 1. Properties and the effects of adrenocorticotropin and fluoride. *J Biol Chem* 244: 3468–3476.

10. Boston BA, Cone RD (1996) Characterization of melanocortin receptor subtype expression in murine adipose tissues and in the 3T3-L1 cell line. *Endocrinology* 137: 2043–2050.
11. Maruyama K, Sugano S (1994) Oligo-capping: a simple method to replace the cap structure of eukaryotic mRNAs with oligoribonucleotides. *Gene* 138: 171–174.
12. Schaefer BC (1995) Revolution in rapid amplification of cDNA ends: new strategies for polymerase chain reaction cloning of full-length cDNA ends. *Anal Biochem* 227: 255–273.
13. Grunfeld C, Baird K, Van Obberghen E, Kahn CR (1981) Glucocorticoid-induced insulin resistance in vitro: evidence for both receptor and postreceptor defects. *Endocrinology* 109: 1723–1730.
14. Cammas FM, Pullinger GD, Barker S, Clark AJL (1997) The mouse adrenocorticotropin receptor gene: cloning, characterization of its promoter and evidence for a role for the orphan nuclear receptor steroidogenic factor 1. *Mol Endocrinol* 11: 867–876.
15. Naville D, Jaillard C, Barjhoux L, Durand P, Begeot M (1997) Genomic structure and promoter characterization of the human ACTH receptor gene. *Biochem Biophys Res Comm* 230: 7–12.
16. Sarkar D, Kambe F, Hayashi Y, Ohmori S, Funahashi H, Seo H (2000) Involvement of AP-1 and steroidogenic factor (SF)-1 in the cAMP-dependent induction of human adrenocorticotropin hormone receptor (ACTHR) promoter. *Endocr J* 47: 63–75.
17. MacDougald OR, Lane MD (1995) Transcriptional regulation of gene expression during adipocyte differentiation. *Ann Rev Biochem* 64: 345–373.
18. Magenis RE, Smith L, Nadeau JH, Johnson KR, Mountjoy KG, Cone RD (1994) Mapping of the ACTH, MSH, and neural (MC3 and MC4) melanocortin receptors in the mouse and human. *Mamm Genome* 8: 503–508.

# Unexpected role of TNF- $\alpha$ in graft versus host reaction (GVHR): donor-derived TNF- $\alpha$ suppresses GVHR via inhibition of IFN- $\gamma$ -dependent donor type-1 immunity

Satoshi Yamamoto<sup>1,2</sup>, Takemasa Tsuji<sup>1</sup>, Junko Matsuzaki<sup>1</sup>, Yue Zhange<sup>1</sup>, Kenji Chamoto<sup>1</sup>, Akemi Kosaka<sup>1</sup>, Yuji Togashi<sup>1</sup>, Kenji Sekikawa<sup>3</sup>, Ken-ichi Sawada<sup>2</sup>, Tsuguhide Takeshima<sup>1</sup>, Takao Koike<sup>2</sup> and Takashi Nishimura<sup>1</sup>

<sup>1</sup>Division of Immunoregulation, Institute for Genetic Medicine and <sup>2</sup>Department of Internal Medicine II, School of Medicine, Hokkaido University, Sapporo, Japan

<sup>3</sup>National Institute of Animal Health, Tsukuba, Japan

**Keywords:** CTL, cytokines, graft vs host disease, Th1/Th2 cells, transplantation

## Abstract

Graft versus host disease (GVHD) is a major complication of allogeneic hematopoietic stem cell transplantation, leading to significant morbidity and mortality. Host-derived TNF- $\alpha$  play a role in the induction of allo-reactive donor T cell activation and the pathogenesis of GVHD. On the other hand, the precise role of donor-derived TNF- $\alpha$  in GVHD remains unclear. To elucidate this issue, we designed an acute GVHD model using (B6 $\times$ D2) F1 recipient mice transferred with spleen cells derived from either wild-type or TNF- $\alpha$ <sup>-/-</sup> C57BL/6 mice. Surprisingly, we found that spleen cells from TNF- $\alpha$ <sup>-/-</sup> mice induce more severe graft versus host reaction (GVHR) than wild-type spleen cells upon transfer into B6D2F1 mice. Transplantation of TNF- $\alpha$ <sup>-/-</sup> mouse spleen cells was associated with enhanced anti-host CTL generation and augmented deletion of host cells. Moreover, mice receiving TNF- $\alpha$ <sup>-/-</sup> cells showed significantly higher levels of serum IFN- $\gamma$ , which was mainly produced by donor CD8<sup>+</sup> T cells. We also demonstrated that TNF- $\alpha$  deficiency in donor spleen cells caused a marked elevation of TNF- $\alpha$  producing capacity by LPS-stimulated host macrophages. Such enhanced GVHR was completely prevented by using TNF- $\alpha$ <sup>-/-</sup>IFN- $\gamma$ <sup>-/-</sup> splenic cells. Our findings demonstrate, for the first time, that donor-derived TNF- $\alpha$  suppress GVHR by inhibiting IFN- $\gamma$ -dependent donor type-1 immunity which is essential for host TNF- $\alpha$  elevation.

## Introduction

Allogeneic hematopoietic stem cell transplantation (HST) has been an effective treatment of hematologic malignancies and genetic disorders (1). The success rate of HST has steadily increased in recent years, but graft versus host disease (GVHD) is still a major cause of post-transplantation mortality (2,3). The generation of a strong graft versus host reaction (GVHR) is induced by activated donor T cells which recognize major and/or minor histocompatibility Ag mismatches. Cytokine dysregulation and organ damage due to pre-transplantation conditioning regimens are also involved in the development of GVHR (4–7).

Tumor necrosis factor  $\alpha$  (TNF- $\alpha$ ) has been implicated in the pathogenesis of GVHD. TNF- $\alpha$  induces a direct toxicity to host tissues and enhances the expression of MHC (8) and

adhesion molecules (9). Moreover TNF- $\alpha$  may act as an autocrine T cell growth factor (10) and thus augment donor T cell clonal expansion. Anti-TNF- $\alpha$  mAb can ameliorate the severity of GVHD (11–13). In a recent study, it was shown that TNF- $\alpha$ R p55 of the recipient controls early GVHD (14) and that TNF- $\alpha$ R p55 of the donor plays a critical role in allo-reactive T cell response (15). Therefore, recipient-derived TNF- $\alpha$  contributes to the activation of allo-reactive T cells and augments the severity of acute GVHD. In contrast, the role of donor-derived TNF- $\alpha$  in GVHD remains unclear.

In the present study, we have examined the role of donor-derived TNF- $\alpha$  in allo-reactive T cell responses *in vivo* using well-characterized mouse models of GVHD. We demonstrate that mice transferred with TNF- $\alpha$ -deficient mouse spleen cells

Correspondence to: T. Nishimura; E-mail: tak24@igm.hokudai.ac.jp

Transmitting editor: T. Saito

Received 9 January 2004, accepted 4 March 2004

exhibit augmented general parameters associated with GVHR, including early elevation of donor-derived IFN- $\gamma$ , generation of anti-host CTL and producing host-derived TNF- $\alpha$ . These data document an unrecognized role of donor-derived TNF- $\alpha$ , which might suppress early GVHR through the control of IFN- $\gamma$ -dependent donor type-1 immunity.

## Methods

### *Mice*

C57BL/6J (B6) (H-2<sup>b</sup>) and B6  $\times$  DBA/2 F1 (B6D2F1) mice were obtained from Charles River Japan (Yokohama, Japan), TNF- $\alpha$ <sup>-/-</sup> C57BL/6 mice were provided by Dr K. Sekikawa (Department of Immunology, National Institute of Animal Health, Tsukuba, Japan) and IFN- $\gamma$ <sup>-/-</sup> C57BL/6 mice were provided by Dr Y. Iwakura (Institute of Medical Science, University of Tokyo, Tokyo, Japan). 6–10 week-old mice were used for all experiments.

### *Induction of GVHD*

Single-cell suspensions from the spleens of B6 and B6D2F1 mice were prepared in RPMI 1640 medium (Gibco-BRL, Grand Island, NY). The cells were suspended in PBS. Acute GVHD was induced by injecting B6 spleen cells ( $5 \times 10^7$ ) into B6D2F1 mice. Age-matched B6D2F1 mice transferred with syngeneic spleen cells ( $5 \times 10^7$ ) were used as control mice.

### *Flow cytometric analysis*

The phenotypic characterization of spleen cells by flow cytometry was carried out using a FACSCalibur instrument and CELLQuest software (Becton Dickinson, San Jose, CA). mAbs used in these experiments [phycoerythrin (PE)-conjugated anti-CD4 mAb, PE-conjugated anti-CD8 mAb, PE-conjugated anti-B220 mAb and fluorescein isothiocyanate (FITC)-conjugated H-2K<sup>d</sup> mAb] were purchased from PharMingen (San Diego, CA).

### *Intracellular cytokine expression*

For the detection of cytoplasmic cytokine expression, cells stimulated with immobilized anti-CD3 mAb for 6 h in the presence of Brefeldin A were first stained with PerCP-conjugated anti-CD4 mAb or cyochrome-conjugated anti-CD8 mAb and FITC-conjugated anti-H-2K<sup>d</sup> mAb, fixed with 4% paraformaldehyde and treated with permeabilizing solution (50 mM NaCl, 5 mM EDTA, 0.02% NaN<sub>3</sub> and 0.5% Triton X-100, pH 7.5). The fixed cells were then stained with PE-conjugated anti-IFN- $\gamma$  mAb for 45 min on ice. The percentage of cells expressing cytoplasmic IFN- $\gamma$  was determined by flow cytometry (FACSCalibur). PerCP-conjugated anti-CD4 mAb, cyochrome-conjugated anti-CD8 mAb and PE-conjugated anti-IFN- $\gamma$  mAb were purchased from PharMingen.

### *Cytotoxicity assay*

The cytotoxicity mediated by CTL was measured by 4 h <sup>51</sup>Cr-release assay as described previously (16). H-2K<sup>d</sup> specific cytotoxicity was determined using DBA/2-derived P815 mastocytoma cells (H-2K<sup>d</sup>) as target cells. As control, C57BL/6-derived MBL-2 T lymphocyte cells (H-2K<sup>b</sup>) were used. The

percentage cytotoxicity was calculated as described previously (16).

### *Generation of CTL in mixed lymphocyte culture (MLC)*

Spleen cells ( $5 \times 10^6$  cells) from GVHD mice and control mice were co-cultured with BDF1 mouse spleen cells ( $2.5 \times 10^6$  cells) which were inactivated by pretreatment with mitomycin C (60  $\mu$ g/ml; Kyowa Hakko Kogyo, Tokyo, Japan). Cells were co-cultured for 4 days in flat-bottomed 12-well plates. After culture, cells were harvested and their cytotoxicity was measured.

### *Measurement of cytokine levels by ELISA*

IFN- $\gamma$  levels in serum or culture supernatants were evaluated with commercial ELISA kit (Amersham International, Buckinghamshire, UK) according to the manufacturer's instructions.

### *Measurement of serum TNF- $\alpha$ levels induced by LPS injection*

LPS-induced TNF- $\alpha$  production was assayed in mice transferred with spleen cells from wild-type or TNF- $\alpha$ <sup>-/-</sup> mouse spleen cells. As a control, B6D2F1 mice transferred with syngeneic mouse spleen cells were used. Ten days after GVHR induction, the mice were treated with or without i.v. injection of LPS (10  $\mu$ g) and their serum samples were harvested 90 min after LPS injection to determine serum TNF- $\alpha$  levels by ELISA (Amersham).

### *Statistical analysis*

Difference between the means of experimental groups were analyzed using the Student's *t*-test. Differences were considered significant where *P* < 0.05.

## Results

### *TNF- $\alpha$ deficiency in donor cells accelerates GVHR in mice*

B6D2F1 (H-2<sup>d</sup>) mice were treated with i.v. injection of wild-type or TNF- $\alpha$ <sup>-/-</sup> C57BL/6 (H-2<sup>b</sup>) spleen cells. As a control, mice were injected with syngeneic B6D2F1 spleen cells. After 14 days, mice were sacrificed to examine the frequency of host cell deletion, as detected with anti-H-2<sup>d</sup> mAbs and flow cytometry. As shown in Fig. 1, in mice transferred with wild-type C57BL/6 mouse spleen cells the percentage of host B cells decreased to 28.7%. Deletion of host B cells was further enhanced (84.3%) when TNF- $\alpha$ <sup>-/-</sup> mouse spleen cells were transferred into B6D2F1 mice. Host cell deletion was also demonstrated among CD4<sup>+</sup> and CD8<sup>+</sup> T cells (data not shown). Consistent with these findings, spleen cells obtained from B6D2F1 mice treated with TNF- $\alpha$ <sup>-/-</sup> splenocytes exhibited higher levels of anti-host CTL activity compared with spleen cells from mice transferred with control (B6D2F1) or wild-type C57BL/6 mouse splenocytes (Fig. 2).

### *TNF- $\alpha$ deficiency in donor cells accelerates the elevation of serum IFN- $\gamma$ levels initiated by donor type-1 immunity during GVHD*

As previously described (17,18), type-1 cytokines such as IL-12 and IFN- $\gamma$  play a critical role in acute GVHD induction.

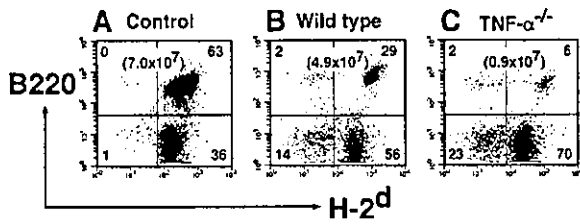


**Fig. 1.** Acceleration of host B cell deletion by GVH response in mice transferred with TNF- $\alpha^{-/-}$  spleen cells. GVH response was induced in BDF1 mice by cell transfer with (A) syngeneic BDF1 (H-2<sup>b</sup>) spleen cells, (B) wild-type C57BL/6 (H-2<sup>b</sup>) spleen cells or (C) TNF- $\alpha^{-/-}$  C57BL/6 (H-2<sup>b</sup>) spleen cells as described in Methods ( $n = 6$ ). Fourteen days after GVH induction, host B cell deletion by GVHD response was determined by flow cytometry after staining with PE-labeled anti-B220 mAb and FITC-labeled anti-H-2K<sup>d</sup> mAb. The numbers represent the percentage of cells in spleen cells. The total cell numbers of B cells in spleen is indicated in parentheses. Similar results were obtained in three different experiments.

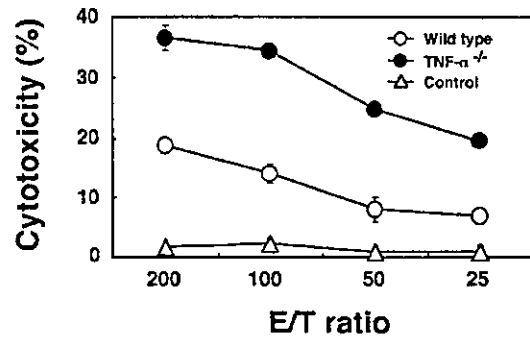


**Fig. 2.** Augmentation of anti host CTL generation in mice transferred with TNF- $\alpha^{-/-}$  spleen cells. BDF1 recipient mice were transferred with BDF1 mouse spleen cells (closed triangle), wild-type C57BL/6 (open circle) or TNF- $\alpha^{-/-}$  C57BL/6 (closed circle) spleen cells. After 14 days, spleen cells were harvested from all mice and their CTL activity against host type P815 mastocytoma cells was measured by 4 h <sup>51</sup>Cr-release assay. The data represent mean  $\pm$  SE of three mice. Similar results were obtained in three different experiments.

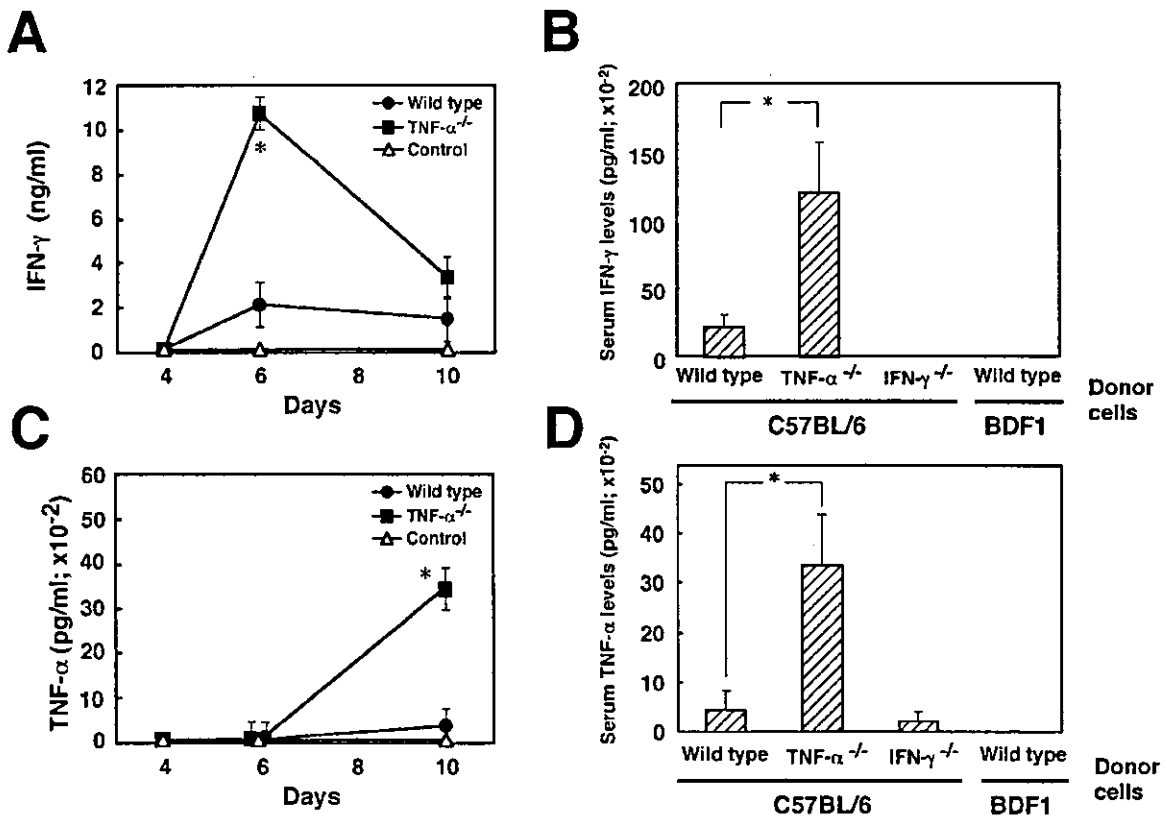


**Fig. 3.** TNF- $\alpha^{-/-}$  mice exhibited augmented producing ability of IFN- $\gamma$  and TNF- $\alpha$  during GVHD. (A and B) Serum IFN- $\gamma$  levels induced by allogeneic TNF- $\alpha^{-/-}$  spleen cells during GVHD. BDF1 recipient mice were transferred with syngeneic BDF1, wild-type C57BL/6, TNF- $\alpha^{-/-}$  C57BL/6 or IFN- $\gamma^{-/-}$  C57BL/6 spleen cells. (A), After 2, 6 or 10 days, serum IFN- $\gamma$  levels of all mice were measured by ELISA. (B) Serum IFN- $\gamma$  levels 6 days after donor cell transfer. (C and D) LPS-induced TNF- $\alpha$  production in recipient mice transferred with allogeneic TNF- $\alpha^{-/-}$  spleen cells. BDF1 recipient mice were transferred with syngeneic BDF1, wild-type C57BL/6, TNF- $\alpha^{-/-}$  C57BL/6 or IFN- $\gamma^{-/-}$  spleen cells. (C) After 2, 6 or 10 days, the recipient mice were treated with i.v. injection of LPS (10  $\mu$ g/mouse) and their serum TNF- $\alpha$  level was determined by ELISA 90 min after LPS injection. (D) LPS-induced serum TNF- $\alpha$  elevation 10 days after donor cell transfer. The data represent mean  $\pm$  SE of three mice. Similar results were obtained in three different experiments. \* $P < 0.05$ .

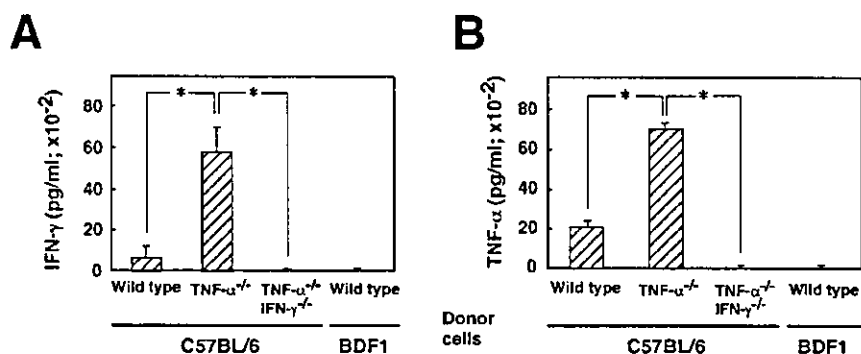


**Fig. 4.** Requirement of donor-derived IFN- $\gamma$  for enhanced elevation of serum IFN- $\gamma$  and TNF- $\alpha$  in mice injected with allogeneic TNF- $\alpha^{-/-}$  spleen cells. B6D2F1 recipient mice were transferred with syngeneic BDF1, wild-type C57BL/6, TNF- $\alpha^{-/-}$  C57BL/6 or TNF- $\alpha^{-/-}$ /IFN- $\gamma^{-/-}$  C57BL/6 spleen cells. (A) Serum IFN- $\gamma$  levels were determined 7 days after GVH induction. (B) Serum TNF- $\alpha$  levels were measured 90 min after LPS injection into GVH mice at 10 days. The data represent means  $\pm$  SE of three mice. Similar results were obtained in three different experiments. \* $P < 0.05$ .

Therefore, we tested serum IFN- $\gamma$  levels in recipient animals. Serum IFN- $\gamma$  levels in recipient B6D2F1 mice became detectable at 4 days and reached a plateau at 6 days after transfer of wild-type or TNF- $\alpha^{-/-}$  C57BL/6 spleen cells. The kinetics of serum IFN- $\gamma$  production during GVHD is illustrated in Fig. 3(A). B6D2F1 mice transferred with TNF- $\alpha^{-/-}$  spleen cells showed significantly higher levels of IFN- $\gamma$  compared with mice transferred with wild-type C57BL/6 spleen cells. Of note, recipient mice treated with IFN- $\gamma^{-/-}$  C57BL/6 spleen cells did not show any increase in serum IFN- $\gamma$ . This finding indicated that elevation of serum IFN- $\gamma$  levels in recipient mice is dependent on the capacity of donor cells to produce IFN- $\gamma$ .

#### *TNF- $\alpha$ deficiency in donor cells enhances TNF- $\alpha$ production by host cells during GVHD*

It has been reported that the capacity of host cells to produce TNF- $\alpha$  increases during the development of GVHR (19). Therefore, it was of great interest to determine how TNF- $\alpha$  deficiency in donor cells influences TNF- $\alpha$  production by host cells during GVHR. As shown in Fig. 3(C) and (D), we detected an increase of serum TNF- $\alpha$  levels upon injection of lipopolysaccharide (LPS) in B6D2F1 mice 10 days after treatment with wild-type C57BL/6 splenocytes but not B6D2F1 splenocytes. Recipient mice transferred with TNF- $\alpha^{-/-}$  spleen cells, but not IFN- $\gamma^{-/-}$  spleen cells, showed robust elevation of TNF- $\alpha$  levels in response to LPS injection. Thus, these results demonstrate that defective TNF- $\alpha$  production in donor cells unexpectedly increases host TNF- $\alpha$  production. This phenomenon may contribute to the accelerated deletion of host cells observed in recipient animals that were treated with TNF- $\alpha^{-/-}$  splenocytes.

#### *Suppression of GVHR by donor-derived TNF- $\alpha$ is associated with reduced donor type-1 immunity*

As shown in Fig. 3(B) and (D), donor-derived IFN- $\gamma$  appears to be critical for initiation of early GVHR. To understand the precise role of donor-derived IFN- $\gamma$  for enhanced IFN- $\gamma$  and TNF- $\alpha$  production in B6D2F1 mice treated with TNF- $\alpha^{-/-}$  mouse spleen cells, we evaluated TNF- $\alpha^{-/-}$ /IFN- $\gamma^{-/-}$  splenocyte for induction of GVHD in B6D2F1 mice. Consistent with previous results (Fig. 3), we observed a marked elevation of both serum

IFN- $\gamma$  and TNF- $\alpha$  in recipient mice transferred with TNF- $\alpha^{-/-}$  spleen cells. However, no significant IFN- $\gamma$  and TNF- $\alpha$  production was observed when animals received splenocytes from TNF- $\alpha^{-/-}$ /IFN- $\gamma^{-/-}$  mice (Fig. 4). These results suggest that defective TNF- $\alpha$  production by donor cells accelerates GVHR by activating donor IFN- $\gamma$ -dependent type-1 immunity. To determine which subset of donor T cells is responsible for activating type 1 immunity, we examined the IFN- $\gamma$  producing capacity of CD4 $^{+}$  and CD8 $^{+}$  T cells from both donor (H-2 $^{b}$ , H-2 $^{d}$ ) and recipient (H-2 $^{d}$ ) mice by intracellular staining (Fig. 5). In keeping with the results of Fig. 3, B6D2F1 mice treated with TNF- $\alpha^{-/-}$  spleen cells contained a higher frequency of IFN- $\gamma$ -producing donor-derived CD8 $^{+}$  and CD4 $^{+}$  T cells. Donor-derived CD8 $^{+}$  Tc1 cells were particularly activated to produce IFN- $\gamma$  (Fig. 5). In addition to the activation of donor Th1 and Tc1 cells, host Th1 and Tc1 cells were also activated to produce IFN- $\gamma$ . However, when TNF- $\alpha^{-/-}$ /IFN- $\gamma^{-/-}$  spleen cells were used as donor cells, no significant increase of recipient-derived IFN- $\gamma$  producing Th1 and Tc1 cells were induced (Fig. 5).

We further demonstrated that anti-host CTL generation, which is essential for the deletion of host cells, is greatly reduced in B6D2F1 mice transferred with TNF- $\alpha^{-/-}$ /IFN- $\gamma^{-/-}$  spleen cells, as compared with mice transferred with TNF- $\alpha^{-/-}$  spleen cells (Fig. 6). In this experiment, CTL were induced from spleen cells of B6D2F1 mice transferred with donor cells by resensitized with B6D2F1 spleen cells because freshly isolated spleen cells from recipient mice 7 days after donor cell transfer exhibited low levels of cytotoxicity.

Thus, we concluded that in the absence of donor-derived TNF- $\alpha$  during the early phase of GVHR, donor-type-1 immunity, especially Tc1 activity, is activated in a manner that depends on IFN- $\gamma$  production by donor cells. Subsequently, enhanced host type-1 immunity may induce TNF- $\alpha$  production by host macrophages, which in turn augments GVHR.

## Discussion

In the present paper, we clarify the precise role of donor-derived TNF- $\alpha$  in acute GVHD using donor spleen cells from TNF- $\alpha^{-/-}$  mice. We find that the defects in donor-derived TNF- $\alpha$

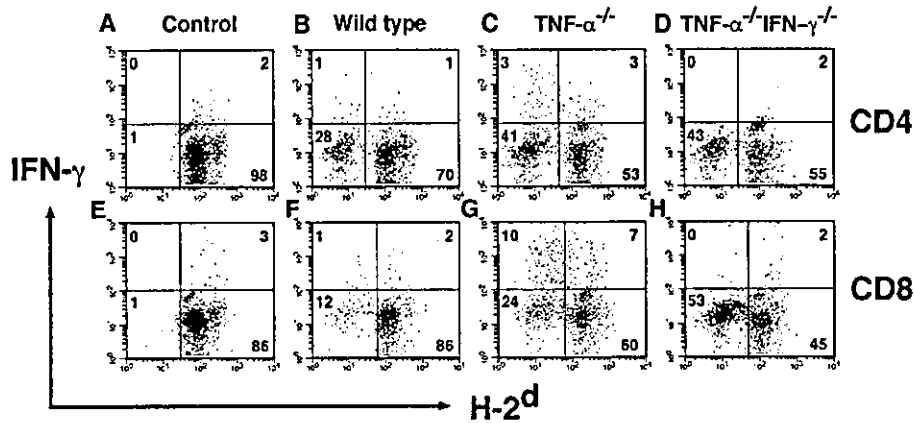


**Fig. 5.** Induction of donor-derived IFN- $\gamma$ -producing CD4<sup>+</sup> and CD8<sup>+</sup> T cells by allogeneic TNF- $\alpha$ <sup>-/-</sup> spleen cells. BDF1 recipient mice were transferred with syngeneic BDF1 (A and E), wild-type C57BL/6 (B and F), TNF- $\alpha$ <sup>-/-</sup> C57BL/6 (C and G) or TNF- $\alpha$ <sup>-/-</sup>IFN- $\gamma$ <sup>-/-</sup> spleen cells (D and H). After 7 days, spleen cells were prepared from all mice and their intracellular cytokine expression profile was examined by flow cytometry. (A–D) Expression profile of CD4<sup>+</sup> T cells; (E–H) expression profile of CD8<sup>+</sup> T cells. x and y axes indicate H-2<sup>d</sup> and IFN- $\gamma$  expression, respectively. Similar results were obtained in three different experiments.

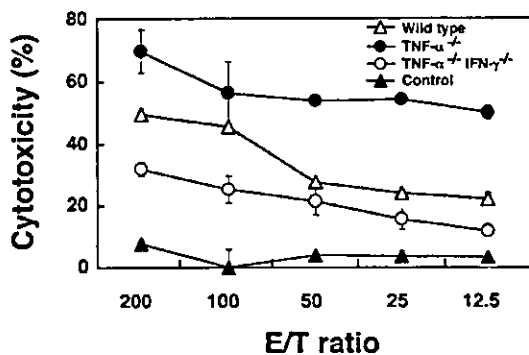


**Fig. 6.** Requirement of IFN- $\gamma$  for enhanced generation of anti-host CTL responses in mice treated with allogeneic TNF- $\alpha$ <sup>-/-</sup> spleen cells. BDF1 recipient mice were transferred with syngeneic BDF1, wild-type C57BL/6, TNF- $\alpha$ <sup>-/-</sup> C57BL/6 or TNF- $\alpha$ <sup>-/-</sup>IFN- $\gamma$ <sup>-/-</sup> C57BL/6 spleen cells. After 7 days, spleen cells obtained from all mice were cocultured with MMC-treated BDF1 spleen cells and their cytotoxicity against P815 mastocytoma was determined by 4 h <sup>51</sup>Cr-release assay. The data represent means  $\pm$  SE of three mice. Similar results were obtained in three different experiments.

accelerate GVHR, including host IFN- $\gamma$  and TNF- $\alpha$  production. These data suggest that donor-derived TNF- $\alpha$  may suppress GVHR via controlling donor IFN- $\gamma$ -dependent type I immunity.

The critical role of proinflammatory cytokines, particularly TNF- $\alpha$  in acute GVHD, has been described in many experimental models and clinical experiments (20–22). The relationship between pre-transplant conditioning regimens, TNF- $\alpha$  production (22–25) and acute GVHD is particularly well-characterized. Chemotherapy and/or total body irradiation damages host tissues including the skin, intestine and liver. Subsequently, the damaged tissues themselves produce TNF- $\alpha$  and LPS, which leak into the systemic circulation and stimulate residual macrophages in the recipient to produce

TNF- $\alpha$ . Using TNF- $\alpha$  receptor-deficient mice, it has been demonstrated that host-derived TNF- $\alpha$  plays a critical role in the early activation of allo-reactive donor T cells and increases morbidity and mortality of acute GVHD. In mouse models, anti-TNF- $\alpha$  mAb treatment of lethally irradiated recipients early in bone marrow transplantation reduces mortality and ameliorates pathology in skin and gut lesions. Thus, host-derived TNF- $\alpha$  has been considered to play a critical role in acute GVHD. In our present study we observed paradoxical effects indicating that donor-derived TNF- $\alpha$  suppresses early activation of allo-reactive donor T cells. We found that recipients transferred with TNF- $\alpha$ <sup>-/-</sup> spleen cells exhibit higher production of IFN- $\gamma$  by donor Tc1 and Th1 cells, followed by enhanced IFN- $\gamma$  secretion from residual recipient CD4<sup>+</sup> and CD8<sup>+</sup> T cells. Activated donor Tc1 and Th1 cells induce host tissue damage by activating host TNF- $\alpha$ -producing macrophages. Thus, TNF- $\alpha$  deficiency in donor cells accelerates the induction of anti-host CTL activity and host TNF- $\alpha$ -producing capacity, which induces severe GVHR. The augmented IFN- $\gamma$  production is not derived from the different immunological condition between TNF- $\alpha$ -deficient and wild-type mice. TNF- $\alpha$ <sup>-/-</sup> mice possess the same percentage of immunoregulatory cells (CD4<sup>+</sup> Th, CD8<sup>+</sup> Tc and B cells) and exhibit the same levels of T cell responses induced by stimulation with anti-CD3 mAb or alloantigen (data not shown).

To explain our finding, several possible mechanisms are considered as follows: (1) TNF- $\alpha$ <sup>-/-</sup> mice produce higher levels of IFN- $\gamma$  because they produce less amounts of soluble TNF- $\alpha$  receptor (TNF- $\alpha$ R), which is a blockade for TNF- $\alpha$ , in comparison with wild-type mice; and (2) TNF- $\alpha$  produced by activated T cells or APC has a capability of suppressing hyperactivity of T cells. In terms of soluble TNF- $\alpha$  R production, it was demonstrated TNF- $\alpha$ <sup>-/-</sup> mice produced the same levels of soluble TNF- $\alpha$  R2 as wild-type mice when they were injected with LPS (data not shown). This result is consistent with previous report that demonstrated the shedding of TNF- $\alpha$  R was induced independently on TNF- $\alpha$  levels (26). Therefore,



it appears to be unlikely that augmented GVHD is derived from the defect of TNF- $\alpha$  R production in TNF- $\alpha^{-/-}$  mice. TNF- $\alpha^{-/-}$  mice exhibit the same levels of T cell responses to anti-CD3 mAb and alloantigen as wild-type mice (data not shown). This observation suggests that TNF- $\alpha$  produced in wild-type mice does not suppress naive T-cell response to antigen. However, recently, we found that TNF- $\alpha^{-/-}$  mice exhibited greatly enhanced T-cell responses in secondary allogeneic responses compared with wild-type mice, if pre-immunized mouse spleen cells were used as responder cells of MLC (data not shown). These findings strongly suggest that TNF- $\alpha$  may act as a negative feedback factor for T-cell hyperactivity as IL-27 does (27).

As classical risk factors of acute GVHD, HLA mismatches between donor and recipient are well-documented (28,29). Many studies have examined risk factors by studying the production of inflammatory cytokines. Holler *et al.* (30) have demonstrated that host-related secretion of TNF- $\alpha$  during pre-transplant conditioning correlates with subsequent GVHD and mortality after transplantation. Analysis of clinical risk factors for enhanced TNF- $\alpha$  response suggested a role for endogenous endotoxin and immunogenetic factors of cytokine activation. In human, the gene encoding TNF- $\alpha$  is located within the MHC locus on chromosome 6 (31), and the inducibility of TNF- $\alpha$  has been associated with certain HLA-class II genotypes (32). A close association between cytokine gene polymorphisms and cytokine inducibility has also been identified. There is a single base polymorphism in the TNF- $\alpha$  gene at position -308(G/A) (33). The rare allele TNF2(A) is closely associated with HLA A1, B8 and DR3 (34). When allelic distribution of this polymorphism was analyzed in 72 BMT recipients, a clear association of the TNF2(A) allele with enhanced *in vitro* TNF- $\alpha$  production in response to LPS and subsequent development of acute GVHD was noted (35). Another study has reported that the d3 homozygous allele of the TNF- $\alpha$  microsatellite is preferentially associated with grade III/IV GVHD (36). While these data indicate a role for TNF- $\alpha$  production by the recipient in predicting the development of GVHD, the relationship between donor TNF- $\alpha$  production and GVHD severity has never been elucidated. In a mouse model, Cooke *et al.* (37) have reported that LPS responsiveness of donor accessory cells correlates with GVHD severity. These investigators suggested that TNF- $\alpha$  production by LPS-stimulated donor cells may be a risk factor for the development of donor T cell responses to host antigens. In contrast, our data indicate that donor-derived TNF- $\alpha$  has a suppressive effect on the initiation of GVHR. The discrepancy in these results may be due to different cellular sources for TNF- $\alpha$  production. Cooke *et al.* (37) investigated TNF- $\alpha$  producing capacity of LPS-reactive TLR4-bearing APC populations using C3H/HeJ TLR4-deficient mice, while we assessed TNF- $\alpha$  producing ability of donor T cells in addition to APC. We found that accelerated GVHR induced by transfer with TNF- $\alpha^{-/-}$  spleen cells was abrogated when either CD4 $^{+}$  T cells or CD8 $^{+}$  T cells were eliminated from donor spleen cells (data not shown). This result indicates a critical role of T cells in the initiation of GVHR, which might be triggered independently of donor APC populations. Our finding that (i) donor TNF- $\alpha^{-/-}$ IFN- $\gamma^{-/-}$  cells do not accelerate GVHD (Figs 4–6) and (ii) donor-derived CD8 $^{+}$  T cells are major IFN- $\gamma$ -producing T cells during the early

stage of GVHR (Fig. 6), strongly suggests that memory-type IFN- $\gamma$  producing CD8 $^{+}$  T cells play a critical role in GVHR induction. We are currently investigating the detailed cellular mechanisms by which donor-derived TNF- $\alpha$  suppressed donor type-1 immunity.

Donor lymphocyte infusion (DLI) has been frequently utilized for treatment of recurrent hematologic malignancies after allo-HST (38). This procedure re-induces complete remission in many patients, but the risk of lethal GVHD is still hard to predict. Because DLI is performed after primary allo-HST, TNF- $\alpha$  production by damaged tissues in the host after conditioning therapy is not as high as compared with donor-derived TNF- $\alpha$ . At present, it may be of great importance to investigate whether severity of GVHD can be predicted by examining donor TNF- $\alpha$  producing capacity, especially by T cells. We are currently investigating this issue.

In conclusion, we have shown, for the first time, that TNF- $\alpha^{-/-}$  donor cells accelerate GVHR early after allogeneic transplantation. Therefore, donor-derived TNF- $\alpha$  may suppress GVHD morbidity. These findings provide novel approaches to detect patients undergoing allo-HST with increased risk for GVHD. Further studies will be required to determine the role of donor-derived TNF- $\alpha$  in a clinical transplantation setting.

#### Acknowledgements

We would like to thank Dr Luc Van Kaer (Vanderbilt University School of Medicine, Nashville, TN) for reviewing this paper. We thank Ms Shinobu Miyamoto for secretarial assistance. This work was supported in part by a grant-in-aid for Science Research on Priority Areas, Scientific Research (B) and Millennium Project from the Ministry of Education, Science, Technology, Sports, and Culture with the Long-Range Research Initiative Project of Japan Chemical Industry Association.

#### Abbreviations

DLI	donor lymphocyte infusion
GVHD	graft versus host disease
GVHR	graft versus host reaction
HST	hematopoietic stem cell transplantation

#### References

- Martin, P. J., Hansen, J. A., Storb, R. and Thomas, E. D. 1987. Human marrow transplantation: an immunological perspective. *Adv. Immunol.* 40:379.
- Ferrara, J. and Deeg, H. 1991. Graft-versus-host disease. *N. Engl. J. Med.* 324:667.
- Vogelsang, G. B. and Hess, A. D. 1994. Graft-versus-host disease: new directions for a persistent problem. *Blood* 84:2061.
- Slavin, R. E. and Santos, G. W. 1973. The graft-versus-host reaction in man after bone marrow transplantation: pathology, pathogenesis, clinical features and implication. *Clin. Immunol. Immunopathol.* 1:472.
- Storb, R. and Thomas, E. D. 1985. Graft-versus-host-disease in dog and man: the Seattle experience. *Immunol. Rev.* 88:215.
- Allen, R. D., Staley, T. A. and Sidman, C. L. 1993. Differential cytokine expression in acute and chronic murine graft-versus-host disease. *Eur. J. Immunol.* 23:333.
- Xun, C. Q., Thompson, J. S., Jennings, C. D., Brown, S. A. and Widmer, M. B. 1994. Effect of total body irradiation, busulfan-cyclophosphamide, or cyclophosphamide conditioning on inflammatory cytokine release and development of acute and chronic graft-vs-host disease in H-2-incompatible transplanted SCID mice. *Blood* 83:2360.

- 8 Leeuwenberg, J. F., Damme, J. V., Meager, T., Jeunhomme, T. M. and Buurman, W. A. 1988. Effects of tumor necrosis factor on the interferon-gamma-induced major histocompatibility complex class II antigen expression by human endothelial cells. *Eur. J. Immunol.* 18:1469.
- 9 Norton, J. and Sloane, J. P. 1991. ICAM-1 expression on epidermal keratinocytes in cutaneous graft-vs-host disease. *Transplant* 51:1203.
- 10 McKenzie, J. L., Calder, V. L., Starling, G. C. and Hart, D. N. 1995. A role of tumor necrosis factor-alpha in dendritic cell-mediated primary mixed leukocyte reactions. *Bone Marrow Transplant* 15:163.
- 11 Herve, P., Flesch, M., Tiberghien, P., Wijdenes, J., Racadot, E., Bordigoni, P., Plouvier, E., Stephan, J. L., Bourdeau, H. and Holler, E. 1992. Phase I-II trial of a monoclonal anti-tumor necrosis factor alpha antibody for the treatment of refractory severe acute graft-versus-host disease. *Blood* 79:3362.
- 12 Piguet, P. F., Grau, G. E., Allet, B. and Vassalli, P. 1987. Tumor necrosis factor/cachectin is an effector of skin and gut lesions of the acute phase of graft-vs-host disease. *J. Exp. Med.* 166:1280.
- 13 Hattori, K., Hirano, T., Miyajima, H., Yamakawa, N., Tateno, M., Oshimi, K., Kayagaki, N., Yagita, H. and Okumura, K. 1998. Differential effects of anti-Fas ligand and anti-tumor necrosis factor alpha antibodies on acute graft-versus-host disease pathologies. *Blood* 91:4051.
- 14 Speiser, D. E., Bachmann, M. F., Frick, T. W., McKall-Faienza, K., Griffiths, E., Pfeffer, K., Mak, T. W. and Ohashi, P. S. 1997. TNF receptor p55 controls early acute graft-versus-host disease. *J. Immunol.* 158:5185.
- 15 Hill, G. R., Teshima, T., Rebel, V. I., Krijanovski, O. I., Cooke, K. R., Brinson, Y. S. and Ferrara, J. L. 2000. The p55 TNF- $\alpha$  receptor plays a critical role in T cell alloreactivity. *J. Immunol.* 164:656.
- 16 Nishimura, T., Iwakabe, K., Sekimoto, M., Ohmi, Y., Yahata, T., Nakui, M., Sato, T., Habu, S., Tashiro, H., Sato, M. and Ohta, A. 1999. Distinct role of antigen-specific T helper type 1 (Th1) and Th2 cells in tumor eradication *in vivo*. *J. Exp. Med.* 190:617.
- 17 Yabe, M.-Y., Yabe, H., Hattori, K., Shimizu, T., Matsumoto, M., Morimoto, T., Yasuda, Y., Inoue, H., Kato, S. and Nishimura, T. 1999. Role of interleukin-12 in the development of acute graft-versus-host disease in bone marrow transplant patients. *Bone Marrow Transplant* 24:29.
- 18 Nishimura, T., Sadata, A., Yahagi, C., Santa, K., Otsuki, K., Watanabe, K., Yahata, T. and Habu, S. 1996. The therapeutic effect of IL-12 or its antagonist in transplantation immunity. Interleukin 12: cellular and molecular immunology of an important regulatory cytokine. *Ann. N. Y. Acad. Sci.* 795:371.
- 19 Nestel, F. P., Price, K. S., Seemayer, T. A. and Lapp, W. S. 1992. Macrophage priming and lipopolysaccharide-triggered release of tumor necrosis factor  $\alpha$  during graft-versus-host disease. *J. Exp. Med.* 175:405.
- 20 Hill, G. R., Crawford, J. M., Cooke, K. R., Brinson, Y. S., Pan, L. and Ferrara, J. L. 1997. Total body irradiation and acute graft-versus-host disease: the role of gastrointestinal damage and inflammatory cytokines. *Blood* 90:3204.
- 21 Holler, E., Kolb, H. J., Moller, A., Kempeni, J., Liesenfeld, S., Pechumer, H., Lehmacher, W., Ruckdeschel, G., Gleixner, B. and Riedne, C. 1990. Increased serum levels of tumor necrosis factor alpha precede major complications of bone marrow transplantation. *Blood* 75:1011.
- 22 Antin, J. H. and Ferrara, J. L. 1992. Cytokine dysregulation and acute graft-versus-host disease. *Blood* 80:2964.
- 23 Schwaighofer, H., Kernan, N. A., O'Reilly, R. J., Brankova, J., Nachbaur, D., Herold, M., Eibl, B. and Niederwieser, D. 1996. Serum levels of cytokines and secondary messages after T-cell-depleted and non-T-cell-depleted bone marrow transplantation: influence of conditioning and hematopoietic reconstitution. *Transplant* 62:947.
- 24 Remberger, M., Ringden, O. and Markling, L. 1995. TNF alpha levels are increased during bone marrow transplantation conditioning in patients who develop acute GVHD. *Bone Marrow Transplant* 15:99.
- 25 Holler, E., Kolb, H. J., Mittermuller, J., Kaul, M., Ledderose, G., Duell, Th., Seeber, B., Schleuning, M., Hintermeier-Knabe, R., Ertl, B., Kempeni, J. and Wilmanns, W. 1995. Modulation of acute graft-versus-host-disease after allogeneic bone marrow transplantation by tumor necrosis factor alpha (TNF $\alpha$ ) release in the course of pretransplant conditioning: role of conditioning regimens and prophylactic application of a monoclonal antibody neutralizing human TNF alpha (MAK 195F). *Blood* 86:890.
- 26 Carpenter, A., Evans, T. J., Buurman, W. A., Bemelmans, M. H., Moyes, D. and Cohen, J. 1995. Differences in the shedding of soluble TNF receptors between endotoxin-sensitive and endotoxin-resistant mice in response to lipopolysaccharide or live bacterial challenge. *J. Immunol.* 155:2005.
- 27 Villarino, A., Hibbert, L., Lieberman, L., Wilson, E., Mark, T., Yoshida, H., Kastelein, R. A., Saris, C. and Hunter C. A. 2003. The IL-27R (WSX-1) is required to suppress T cell hyperactivity during infection. *Immunity* 19:645.
- 28 Klingemann, H. G., Storb, R., Fefer, A., Deeg, H. J., Appelbaum, F. R., Buckner, C. D., Cheever, M. A., Greenberg, P. D., Stewart, P. S. and Sullivan, K. M. 1986. Bone marrow transplantation in patients aged 45 years and older. *Blood* 67:770.
- 29 Weisdorf, D., Hakke, R., Blazar, B., Miller, W., McGlave, P., Ramsay, N., Kersey, J. and Filipovich, A. 1991. Risk factor for acute graft-versus-host-disease in histocompatible donor bone marrow transplantation. *Transplant* 51:1197.
- 30 Holler, E., Ertl, B., Hintermeier-Knabe, R., Roncarolo, M. G., Eissner, G., Mayer, F., Fraunberger, P., Behrends, U., Pfannes, W., Kolb, H. J. and Wilmanns, W. 1997. Inflammatory reactions induced by pretransplant conditioning—an alternative target for modulation of acute GVHD and complications following allogeneic bone marrow transplantation. *Leuk. Lymphoma* 25:217.
- 31 Carroll, M. C., Katzman, P., Alicot, E. M., Koller, B. H., Geraghty, D. E., Orr, H. T., Strominger, J. L. and Spies, T. 1987. Linkage map of the human major histocompatibility complex including the tumor necrosis factor genes. *Proc. Natl Acad. Sci. USA* 84:8535.
- 32 Jacob, C. O., Fronck, Z., Lewis, G. D., Koo, M., Hansen, J. A. and McDevitt, H. O. 1990. Heritable major histocompatibility complex class II-associated differences in production of tumor necrosis factor: relevance to genetic predisposition to systematic lupus erythematosus. *Proc. Natl Acad. Sci. USA* 87:1233.
- 33 Wilson, A. G., di Giovine, F. S., Blakemore, A. I. and Duff, G. W. 1992. Single base polymorphism in the tumor necrosis factor alpha (TNF $\alpha$ ) gene detectable by NcoI restriction of PCR product. *Hum. Mol. Genet.* 1:353.
- 34 Wilson, A. G., de Vries, N., Pociot, F., di Giovine, F. S., van der Putte, L. B. and Duff, G. W. 1993. An allelic polymorphism within the human tumor necrosis factor  $\alpha$  promoter region is strongly associated with HLA A1, B8 and DR3 alleles. *J. Exp. Med.* 177:557.
- 35 Mayer, F. R., Messer, G., Knabe, H., Memple, W., Meurer, M., Kolb, H. J. and Holler, E. 1996. High response of TNF- $\alpha$  secretion *in vivo* in patients undergoing BMT may be associated with the -308 bp TNF- $\alpha$  gene enhancer-polymorphism. *Bone Marrow Transplant* 17:S101.
- 36 Middleton, P. G., Taylor, P. R., Jackson, G., Proctor, S. J. and Dickinson, A. M. 1998. Cytokine gene polymorphisms associating with severe acute graft-versus-host disease in HLA-identical sibling transplants. *Blood* 92:3943.
- 37 Cooke, K. R., Hill, G. R., Crawford, J. M., Bungard, D., Brinson, Y. S., Delmonte, J. and Ferrara, J. L. 1998. Tumor necrosis factor- $\alpha$  production to lipopolysaccharide stimulation by donor cells predicts the severity of experimental acute graft-versus-host-disease. *J. Clin. Invest.* 102:1882.
- 38 Collins, R. H. Jr, Shpilberg, O., Drobyski, W. R., Porter, D. L., Giralt, S., Champlin, R., Goodman, S. A., Wolff, S. N., Hu, W., Verfaillie, C., List, A., Dalton, W., Ognoskie, N., Chetrit, A., Antin, J. H. and Nemunaitis, J. 1997. Donor leukocyte infusions in 140 patients with relapsed malignancy. *J. Clin. Oncol.* 15:433.

## Progenitor cell mobilization

# Peripheral blood stem cell mobilization following CHOP plus rituximab therapy combined with G-CSF in patients with B-cell non-Hodgkin's lymphoma

T Endo<sup>1</sup>, N Sato<sup>2</sup>, Y Mogi<sup>3</sup>, K Koizumi<sup>1</sup>, M Nishio<sup>1</sup>, K Fujimoto<sup>1</sup>, T Sakai<sup>1</sup>, K Kumano<sup>1</sup>, M Obara<sup>1</sup>, H Ikeda<sup>3</sup> and T Koike<sup>1</sup>

<sup>1</sup>Department of Internal Medicine II, Hokkaido University School of Medicine, Sapporo, Japan; <sup>2</sup>Blood Transfusion Service, Hokkaido University Medical Hospital, Sapporo, Japan; and <sup>3</sup>Hokkaido Red Cross Blood Center, Sapporo, Japan

### Summary:

We mobilized peripheral blood stem cells (PBSC) following CHOP plus rituximab (CHOP-R) therapy, and compared with the findings following CHOP therapy without rituximab. All patients were given G-CSF starting from day 11 after CHOP therapy. Patients in the CHOP-R group ( $n=8$ ) were given rituximab on day 12. Target CD34<sup>+</sup> cells number was collected in a single leukapheresis on day 14, from all the eight patients in the CHOP-R group. PBSC mobilization kinetics, CD34<sup>+</sup> cells yield and colony-forming ability in the graft collection, toxicity during mobilization, and engraftment after transplantation of CHOP-R group were not significantly different from those in the CHOP group ( $n=8$ ). In all patients given CHOP-R therapy, CD20<sup>+</sup> cells and immunoglobulin heavy chain (IgH) rearrangement in the graft collection were undetectable by flow-cytometric analysis and Southern blot analysis, respectively, but with PCR analysis two of eight grafts were positive for IgH rearrangement. While further studies are needed to evaluate the efficacy of purging and the outcome of patients undergoing autologous transplantation, CHOP-R therapy can be safely and effectively used in the mobilization phase of PBSC collection, without excess clinical toxicity or deleterious effect on PBSC mobilization kinetics or engraftment time.

*Bone Marrow Transplantation* (2004) 33, 703–707.  
doi:10.1038/sj.bmt.1704413

Published online 26 January 2004

**Keywords:** CHOP; rituximab; peripheral blood stem cell (PBSC); mobilization

widely used for patients with non-Hodgkin's lymphoma (NHL).<sup>1,2</sup> One major obstacle to APBSCT is peripheral blood (PB) cell involvement with lymphoma cells. Several studies have shown that the reduction of tumor burden *in vivo* and purging of autografts reduce the risk of contamination by lymphoma cells of the graft, and may improve outcome.<sup>3,4</sup> Some strategies to eliminate contaminating lymphoma cells in the graft are being tested, including *in vitro* purging of grafts with monoclonal antibodies and complement,<sup>5</sup> CD34<sup>+</sup> cell selection,<sup>6</sup> and *in vivo* purging of PB.

Rituximab, a highly specific mouse/human chimeric anti-CD20 antibody (Chugai Pharmaceutical Co. Ltd, Tokyo, Japan), has been seen to cause a rapid depletion of PB B-cells.<sup>7</sup> Regimens, such as high-dose cytosine arabinoside,<sup>8,9</sup> HAM (high-dose cytosine arabinoside/mitoxantrone),<sup>10</sup> and DexaBEAM (dexamethasone/BCNU/etoposide/cytosine arabinoside/melphalan),<sup>11</sup> have been used in conjunction with rituximab during mobilization procedures, to obtain tumor-free progenitor cells. Although sufficient numbers of PBSC could be obtained using these regimens, the timing of leukapheresis differed with each case, because decisions were based on measurement of CD34<sup>+</sup> cells or platelet recovery in the PB.

For patients with NHL, CHOP therapy remains the best available combination chemotherapy.<sup>12</sup> We found no published information addressing the kinetics of PBSC and graft acquisition following therapy with CHOP and rituximab, and we wish to report our experience here. The optimum timing of leukapheresis and effects of rituximab on PBSC mobilization, purging, engraftment, and toxicity are discussed.

### Patients and methods

#### Patients

A total of 16 Japanese patients with newly diagnosed B-cell NHL were enrolled in this study between November 2000 and February 2003. The eligibility criteria were as follows: age between 15 and 65 years; a confirmed histologic diagnosis of CD20-positive B-cell NHL (excluding Burkitt's lymphoma and lymphoblastic lymphoma); prognostic index, constructed by Coiffier *et al*,<sup>13</sup> of intermediate or

High-dose chemotherapy followed by autologous peripheral blood stem cell transplantation (APBSCT) has been

Correspondence: Dr T Endo, Department of Internal Medicine II, Hokkaido University School of Medicine, N-15, W-7, Kita-ku, Sapporo 060-8638, Hokkaido, Japan. E-mail: t-endo@fd5.so-net.ne.jp  
Received 26 June 2003; accepted 08 October 2003  
Published online 26 January 2004

high risk, as defined by having at least one of the four following adverse features: (1) elevated serum lactic dehydrogenase (LDH) level, (2) bulky mass >10 cm, (3) advanced stage III or IV according to the Ann Arbor staging classification, (4) two or more extranodal sites: no severe cardiopulmonary, renal, and hepatic dysfunction. Before November 2001, PBSC were mobilized using the CHOP combined with G-CSF without rituximab (CHOP group, *n*=8). After November 2001, when rituximab became available in Japan, PBSC were mobilized using CHOP plus rituximab regimen combined with G-CSF (CHOP-R group, *n*=8). Thus CHOP and CHOP-R groups were sequentially recruited. Characteristics of these two groups are listed in Table 1.

*Premobilization phase*

All patients were given three cycles of biweekly CHOP therapy with G-CSF support as induction chemotherapy prior to mobilization (Table 1). CHOP therapy consisted of cyclophosphamide (CY) 750 mg/m<sup>2</sup> i.v. on day 1, doxorubicin 50 mg/m<sup>2</sup> i.v. on day 1, vincristine 1.4 mg/m<sup>2</sup> i.v. on day 1 (maximal dose, 2 mg), and prednisolone 50 mg/m<sup>2</sup> orally from day 1 to day 5. Patients were given G-CSF (Lenograstim, Chugai Pharmaceutical Co., Tokyo, Japan) at a dose from 1 to 5 μg/kg/day, subcutaneously, starting from the day when the total leukocyte count was <3.0 × 10<sup>9</sup>/l. Thereafter, it was withdrawn when the leukocyte count exceeded 10 × 10<sup>9</sup>/l, and the next cycle of CHOP therapy was immediately started.<sup>14</sup> No patients, including the patients in the CHOP-R group, were given rituximab in the premobilization phase.

**Table 1** Patient characteristics

	CHOP	CHOP-R
No. of patients	8	8
<i>Sex (male/female)</i>		
Male	4	1
Female	4	7
<i>Age</i>		
Median	53	54
Range	31-64	41-60
<i>Histology</i>		
Follicular	1	4
Mantle cell	1	0
Lymphoplasmacytic	0	1
Diffuse large	6	3
<i>Clinical stage</i>		
I	1	0
II	1	0
III	1	1
IV	5	7
<i>Bone marrow involvement</i>		
Yes	1	6
No	7	2
<i>Disease status at PBSC harvest</i>		
CR	4	3
Not CR	4	5

*Mobilization and collection of PBSC*

One or two leukaphereses were performed after the fourth cycle of biweekly CHOP therapy. CY dose was increased to 1000 mg/m<sup>2</sup>. Mobilization and collection of PBSC were scheduled as follows: The first day of leukapheresis after the start of CHOP therapy was fixed on day 14. Until day 10, patients were given G-CSF (lenograstim) in a dose of 1 μg/kg/day, subcutaneously, when the total leukocyte count was <3.0 × 10<sup>9</sup>/l. All patients were given G-CSF in a dose of 5-10 μg/kg/day, subcutaneously, starting from day 11 until the day of the last apheresis.<sup>15</sup> All the eight patients in the CHOP-R group were given rituximab 375 mg/m<sup>2</sup> 2 days before stem cell collection (day 12 of the CHOP regimen). PBSC collections were made on day 14, using either Cobe Spectra (Lakewood, CO, USA) or CS3000 (Baxter-Fenwal Division, Deerfield, IL, USA). A minimum threshold requirement of CD34<sup>+</sup> cells was 1.5 × 10<sup>6</sup> cells/kg.

*In vitro assays*

PB samples for mobilization kinetics analysis of CD34<sup>+</sup> cells were obtained from day 12 to the end of PBSC apheresis. Flow-cytometric (FCM) analysis of CD34<sup>+</sup> cells and colony-forming units-granulocyte/macrophage (CFU-GM) and burst-forming unit-erythrocyte (BFU-E) colony assay allowed for estimation of the number of progenitor cells in the collection. Colony assay was done using serum containing fibrin clots,<sup>16</sup> with 2 U/ml of recombinant human erythropoietin, 50 U/ml of recombinant interleukin 3, 50 ng/ml of recombinant GM-CSF, and 50 ng/ml of recombinant G-CSF, in flat-bottomed, 24-well-tissue culture plates in a 5% CO<sub>2</sub>/95% atmosphere incubator at 37°C for 14 days. The clots were stained with benzidine-hematoxylin, and for identification the colonies were enumerated using the criteria of Clarke and Housman.<sup>17</sup>

*Toxicity during PBSC mobilization*

All adverse reactions were recorded and graded according to National Cancer Institute criteria.

*Transplantation procedure*

Pre-transplant conditioning regimens for all patients consisted of ranimustine (MCNU) 200 mg/m<sup>2</sup> once daily i.v., on days -8 and -3 (total dose 400 mg/m<sup>2</sup>), carboplatin (CBDCA) 300 mg/m<sup>2</sup> once daily i.v. on days -7 to -4 (total dose 1200 mg/m<sup>2</sup>), etoposide (VP-16) 500 mg/m<sup>2</sup> once daily i.v. on days -6 to -4 (total dose 1500 mg/m<sup>2</sup>), and CY 50 mg/kg once daily i.v. on days -3 and -2 (total dose 100 mg/kg) (MCVC regimen).<sup>18</sup> All patients were given G-CSF (5 μg/kg/day subcutaneously) from day +1 until engraftment. All patients in the CHOP-R group were given rituximab 375 mg/m<sup>2</sup> weekly for 3 weeks after engraftment.

*Evaluation of purging*

In the CHOP-R group, the numbers of CD20<sup>+</sup> cells in PB were compared before and after rituximab administration, that is, day 12 and day 14 of the fourth cycle of CHOP